AD-A144 998 EQUALIZATION OF TIME-VARYING DISPERSIVE CHANNELS VIA SEQUENCE ESTIMATION(U) ESL INC SUNNYVALE CA R IBARAKI ET AL. 13 JUL 83 ESL-TM-1642 DNA-TR-81-316 1/1

UNCLASSIFIED DNA001-81-C-0149 F/G 17/2 NL

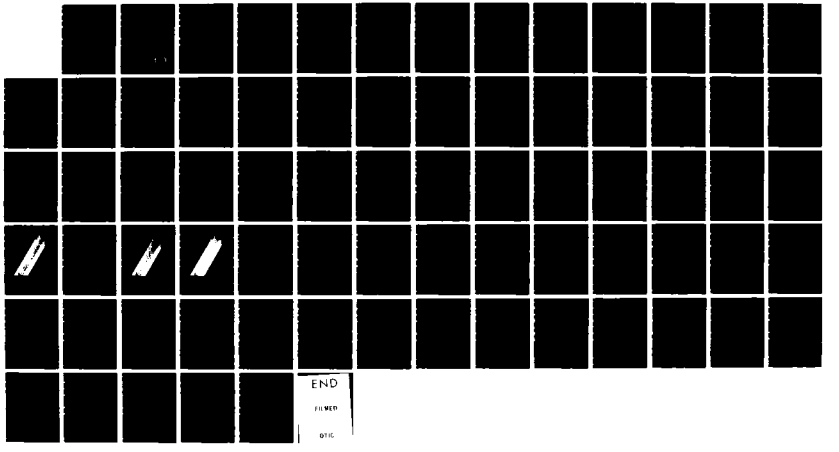

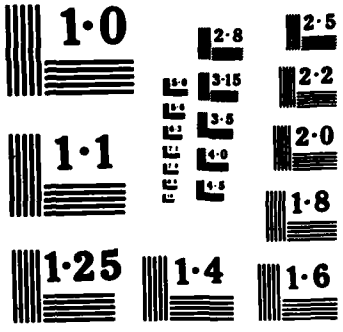
1·0
1·1
1·25
2·8
3·15
3·5
4·0
4·5
2·5
2·2
2·0
1·8
1·4
1·6

DNA-TR-81-316

EQUALIZATION OF TIME-VARYING DISPERSIVE CHANNELS VIA SEQUENCE ESTIMATION

Ronald Y. Ibaraki
Ernest T. Tsui
James E. Hawker
ESL, Incorporated
495 Java Drive
Sunnyvale, California 94086

13 July 1983

Technical Report

CONTRACT No. DNA 001-81-C-0149

THIS WORK WAS SPONSORED BY THE DEFENSE NUCLEAR AGENCY
UNDER RDT&E RMSS CODE B322081466 S99QAXHB00007 H2590D.

Prepared for
Director
DEFENSE NUCLEAR AGENCY
Washington, DC 20305

Destroy this report when it is no longer needed. Do not return to sender.

PLEASE NOTIFY THE DEFENSE NUCLEAR AGENCY, ATTN: STTI, WASHINGTON, D.C. 20305, IF YOUR ADDRESS IS INCORRECT, IF YOU WISH TO BE DELETED FROM THE DISTRIBUTION LIST, OR IF THE ADDRESSEE IS NO LONGER EMPLOYED BY YOUR ORGANIZATION.

UNCLASSIFIED

SECURITY CLASSIFICATION OF THIS PAGE (When Data Entered)

REPORT DOCUMENTATION PAGE	READ INSTRUCTIONS BEFORE COMPLETING FORM
1. REPORT NUMBER: DNA-TR-81-316	2. GOVT ACCESSION NO.: ADA144998
3. RECIPIENT'S CATALOG NUMBER:	
4. TITLE (and Subtitle): EQUALIZATION OF TIME-VARYING DISPERSIVE CHANNELS VIA SEQUENCE ESTIMATION	5. TYPE OF REPORT & PERIOD COVERED: Technical Report
	6. PERFORMING ORG. REPORT NUMBER: ESLTM1642
7. AUTHOR(s): R. Ibaraki, E. Tsui, J. Hawker	8. CONTRACT OR GRANT NUMBER(s): DNA 001-81-C-0149
9. PERFORMING ORGANIZATION NAME AND ADDRESS: ESL, Incorporated, 495 Java Drive, Sunnyvale, California 94086	10. PROGRAM ELEMENT, PROJECT, TASK AREA & WORK UNIT NUMBERS: Task S99QAXHB-00007
11. CONTROLLING OFFICE NAME AND ADDRESS: Director, Defense Nuclear Agency, Washington, D.C. 20305	12. REPORT DATE: 13 July 1983
	13. NUMBER OF PAGES: 72
14. MONITORING AGENCY NAME & ADDRESS(if different from Controlling Office):	15. SECURITY CLASS. (of this report): UNCLASSIFIED
	15a. DECLASSIFICATION/DOWNGRADING SCHEDULE: N/A since UNCLASSIFIED

16. DISTRIBUTION STATEMENT (of this Report)

Approved for public release; distribution unlimited.

17. DISTRIBUTION STATEMENT (of the abstract entered in Block 20, if different from Report)

18. SUPPLEMENTARY NOTES

This work was sponsored by the Defense Nuclear Agency under RDT&E RMSS Code B322081466 S99QAXHB00007 H2590D.

19. KEY WORDS (Continue on reverse side if necessary and identify by block number)

Nuclear Environment
Communications
Frequency-Selective Fading
Channel Equalization

20. ABSTRACT (Continue on reverse side if necessary and identify by block number)

Adaptive maximum likelihood sequence estimation (AMLSE) has been shown to be an effective mitigation technique for high data rate links against the deleterious effects of intersymbol interference resulting from rapidly time-varying and frequency selective fading channels. It was demonstrated that significant performance improvements can be obtained through the use of AMLSE receiver demodulation in comparison to conventional (non-delay spread specialized) receivers and even decision feedback equalization receivers. In addition, several important channel related receiver

DD FORM 1 JAN 73 1473 EDITION OF 1 NOV 65 IS OBSOLETE

UNCLASSIFIED

SECURITY CLASSIFICATION OF THIS PAGE (When Data Entered)

20. ABSTRACT (Continued)

anomalies which introduce symbol timing ambiguities were identified.

TABLE OF CONTENTS

TABLE OF CONTENTS (Continued)

LIST OF ILLUSTRATIONS

LIST OF ILLUSTRATIONS (Continued)

SECTION 1

INTRODUCTION

1.1 BACKGROUND

Frequency selective fading degradation can occur on satellite communication links whose propagation paths are interdicted by structured magnetic field aligned ionization. High megabit symbol rate links are particularly susceptible to the selective fading phenomenon which can cause a significant amount of time delay signal energy spreading, in addition to fading having Rayleigh statistics at each delay. The effect of this energy dispersive channel transfer function is to reduce the received energy per symbol in the normal symbol integration period of conventional receivers and introduce varying intersymbol interference (ISI) which may incorrectly bias the current symbol decision with energy from the other adjacent symbols. Thus, high data rate links which may be designed to operate near the power limit based on the symbol energy-to-noise density ratio E_s/N_o instead become bandwidth limited as a result of the restricted coherence bandwidth.

Some of the alternative courses of action which can be pursued to maintain reliable communications over the selective fading channel are; 1) to reduce the maximum information transmission rate, 2) to use some sort of source encoding or preprocessing to reduce data redundancy or compress the data into a more concise format before transmission, and 3) to use a modem with larger M-ary alphabets (e.g., M-ary FSK or M-ary PSK). An especially attractive alternative which allows the use of the original data rate is to use special receiver processing techniques (i.e., equalization) which are matched to the dispersive

channel to counteract the channel effects and is the subject of this study.

A number of authors have addressed the subject of using recursive adaptive filtering at the receiver to perform conventional channel equalization. Some of the variations include the use of linear transversal filter [2], lattice filters [3], decision-feedback filters [4], and maximum likelihood sequence estimation [5], [6]. Of these four variations, the maximum likelihood sequence estimation (MLSE) technique has demonstrated superior performance [7], and was selected for further investigation in this study. In this adaptive filter variation, a channel estimator (adaptive filter) is used to provide an estimate of the time-varying channel impulse response to a sequence matched filter to compute the best estimates of the transmitted data sequence. The a-posteriori sequence matched filter is efficiently computed via a variation of the Viterbi algorithm (more commonly known as an efficient method of decoding short constraint length convolutional codes).

The time varying frequency selective fading channel, simulated by the DNA Channel Impulse Response Function (CIRF) computer code [1] was used to model the dispersive channel impulse response. This stochastic channel model generates Monte Carlo random sample functions of the channel impulse response based on theoretical power spectral and power delay density descriptions of the selective fading channel.

1.2 OBJECTIVES/OVERVIEW

The objectives of this study was to investigate the feasibility of maximum likelihood sequence estimation as a technique to mitigate the effects of a frequency-selective fading channel. In particular, it

is of interest to determine how well this technique can compensate for the channel induced intersymbol interference which can be viewed as a rate one coding device. In this view, it is of interest to determine whether the signal energy from the multiple independently fading delay paths of a selective fading channel can be combined to achieve a diversity gain over receiver performance in a flat non-selective fading channel. In addition, it will be of interest to identify any potential problems as well as implementation advantages/disadvantages of this adaptive technique.

The report is organized in such a manner as to provide the reader with both a concise summary of results in Section 1.3 (and a brief description of further work in Section 1.4), but also a detailed design description of the various testing and optimization procedures performed in the refinement of the sophisticated sequence estimation equalization technique. Thus, the future investigator will not have to "redo" the preliminary test/optimization procedures to understand how to further improve on the results presented herein.

Section 2 provides a detailed summary of the link models, basic receiver concepts, and the various channel descriptions. The receiver optimization and test results are contained in Sections 3.1 through 3.3. A comparison of sequence estimation with decision feedback techniques for a fixed channel is provided in Section 3.2. The performance of the optimized receiver over a time-varying, dispersive channel are presented in Section 3.4 where lower bounds on attainable performance are presented. Section 3.5 presents a state-of-the-art improvement of the receiver technique using an innovative pre-filter technique and results are presented that show improvements over more conventional techniques.

Finally, Section 3.6 provides performance results of what a "practical" receiver might do under severe channel conditions and discusses how one could implement receiver adaptivity in a straightforward manner.

1.3 SUMMARY AND CONCLUSIONS

1.3.1 Executive Summary

Adaptive maximum likelihood sequence estimation (AMLSE) has been shown to be an effective mitigation technique for high data rate links against the deleterious effects of intersymbol interference resulting from a frequency selective fading channel. It was demonstrated that significant performance improvements can be obtained through the use of AMLSE receiver demodulation in comparison to conventional (non-delay spread specialized) receivers and even decision feedback equalization receivers. In addition, several important channel related receiver anomalies which introduce symbol timing ambiguities were identified.

Previous studies have shown that rapidly varying, frequency-selective fading channels can seriously degrade performance of conventional demodulators. Recently, the application of Decision Feedback Equalization (DFE) has been applied to the trans-ionoshperic scintillation channel with moderate success for relatively mildly selective channels (a few bits of intersymbol interference) and relatively slow fluctuation (approximately 10,000 bits per fade decorrelation time), [11]. The DFE technique also required the implementation of a transmitted training sequence with a 5% overhead penalty to maintain channel lock for the equalizer. The purpose of this report is to present the results of new investigations into an optimal sequence estimation called Adaptive Maximum Likelihood Sequence Estimation (AMLSE). Simulations have shown that very good performance can be obtained for fairly severe selectivity

(approx. ten bits of intersymbol interference) and for fairly rapid fading fluctuations of only 1000 bits per fade decorrelation time. All this performance is obtained potentially without the need for any training sequence whatsoever. The use of a training sequence will only further improve performance.

The AMLSE techniques are somewhat more complex than the DFE techniques but provide significantly better performance especially for severe, rapidly fading channels. An example case run for 1000 bits per decorrelation time and approximately 10 bits pf intersymbol interference resulted in an asymptotic (constant independent of SNR) error rate of approximately 10 per cent for the best DFE design, whereas the AMLSE yielded results below 10^{-3} error rate for 15 to 20 dB SNR depending on the fading record. The reason for the performance improvement apparently lies in the fact that as the channel fluctuation becomes more rapid and the selectivity becomes more severe, the convergence constant and the number of taps of the DFE must be increased proportionately. After a point, given a fixed SNR level, the resultant large convergence constant and large number of taps result in a significant amount of equalizer "misadjustment noise" which essentially causes the taps to wander due to the channel noises. This results in inaccurate equalization and causes a limiting error rate since there is significant residual intersymbol interference that cannot be equalized and becomes "noise" to the receiver.

Simulations of the AMLSE have indicated that although a significant performance potential is present, a problem of occassional bit slippage can occur. Thus, the AMLSE output is essentially error free for the majority of the time but every now and then a bit slip will occur which will cause an error burst due to a misalignment of the output bit sequence. This performance characteristic is highly reminiscent of the Viterbi Decoders used to provide error correction

for convolutionally coded links. In fact, the AMLSE performs the equivalent operation of essentially decoding the channel-caused "code" (i.e., the intersymbol interference) via maximum likelihood decoding implemented via the Viterbi Algorithm. The bit slips are originally caused by the selective channel fading away completely, i.e., all frequencies are faded at the same time just like flat fading. This phenomenon was observed to occur infrequently but when it did occur it caused a burst of errors that often caused the AMLSE to bit slip. In general, if the high data rate link is transmitted via frames, the frame sync (or preamble) bits can be used to "resync" after the bit slip.

Thus, it was found that under mild fading conditions one can use either DFE or AMLSE with comparable performance given comparable implementation complexity however, for rapidly time-varying, severely selective channels AMLSE significantly outperforms DFE techniques.

SECTION 2

2.1 SYSTEM MODEL

A general block diagram of a differentially encoded PSK communication link using an AMLSE receiver and operating in a frequency selective fading (FSF) channel is shown in Figure 2-1. The differentially encoded data stream, c(t), modulates an RF carrier sinusoid and the transmitted signal is given by

$$s(t) = \sqrt{2E_s}\, c(t) \cos(\omega_c t + \theta) \qquad (1)$$

where

c(t) is a sequence of ±1 differentially encoded pulses of the data sequence, d(t),
ω_c is the carrier radian frequency,
E_s is the carrier energy per pulse, and
θ is the transmitted carrier phase.

This BPSK signal is passed through a FSF channel model which imparts a time delay spread of signal energy and adds white Gaussian noise. The receiver front end is modeled as a fixed local oscillator (LO) and mixer followed by in-phase (I) and quadrature (Q) integrate and dump (I&D) filters which provide samples of the received waveform at the channel symbol rate.

The scope of this analysis was restricted to the generation of the intersymbol interference (ISI) channel and the AMLSE demodulation process. Thus, phase or frequency tracking loops, receiver AGC and bit sync circuitry have been assumed to be ideal and have not been simulated.

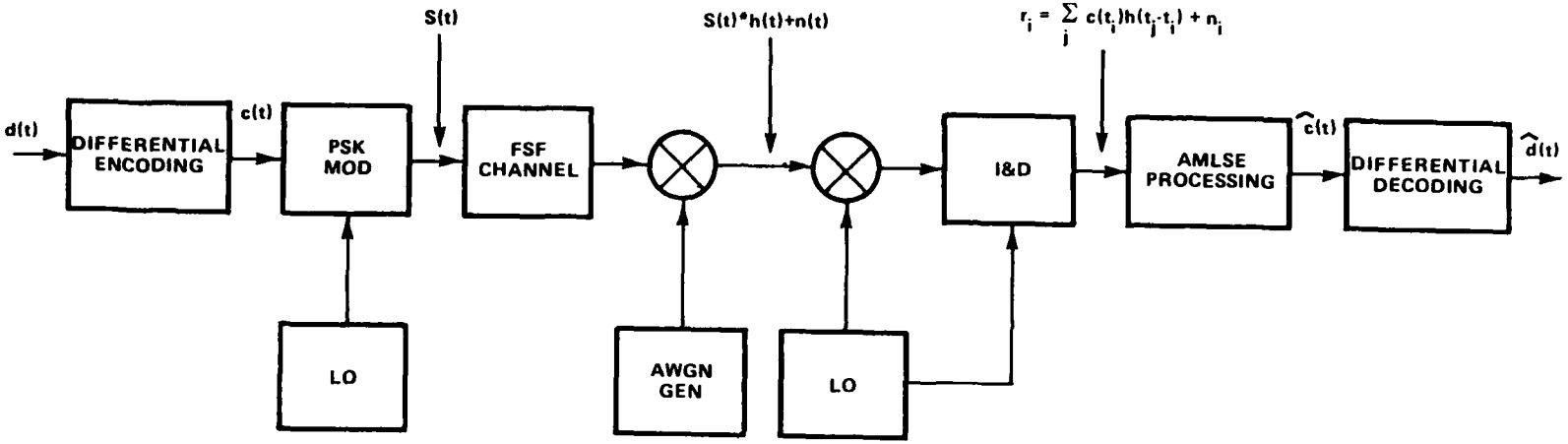

Figure 2-1 General Link Block Diagram

The I&D filter output is sampled at the symbol rate and the complex (I,Q) received signal samples are given by

$$r_k = \sum_j c(t_j)h(t_k - t_j) + n_I(t_k) + n_Q(t_k) \qquad (2)$$

where the summation is the digital convolution of the transmitted symbol sequence with the channel impulse response (complex). The additive white Gaussian-noise (complex) has variance given by

$$E(n_I^2) = E(n_Q^2) = \frac{1}{2\ E_s/N_o} \qquad (3)$$

Figure 2-2 shows the effect of the delay spread channel impulse response convolutions on the transmitted bit or pulse stream (the symbol period for which a demodulation is to take place is indicated by the dashed lines). Note that not only the previous or past symbol(s) interferes with the desired pulse demodulation but the future pulse(s) as well. This occurs since the desired pulse can be significantly spread in delay by the channel to the point that it overlaps future pulses. It is easy to see that when the intersymbol interference is severe its effects can dominate over the additive noise and effectively limit the achievable error rate (independent of SNR!). Under severe ISI conditions, clearly every bit interferes with many others and a bit sequence matched filter will outperform a single bit matched filter. This intuitive observation leads one to evaluate an optimum sequence demodulation method to be discussed below.

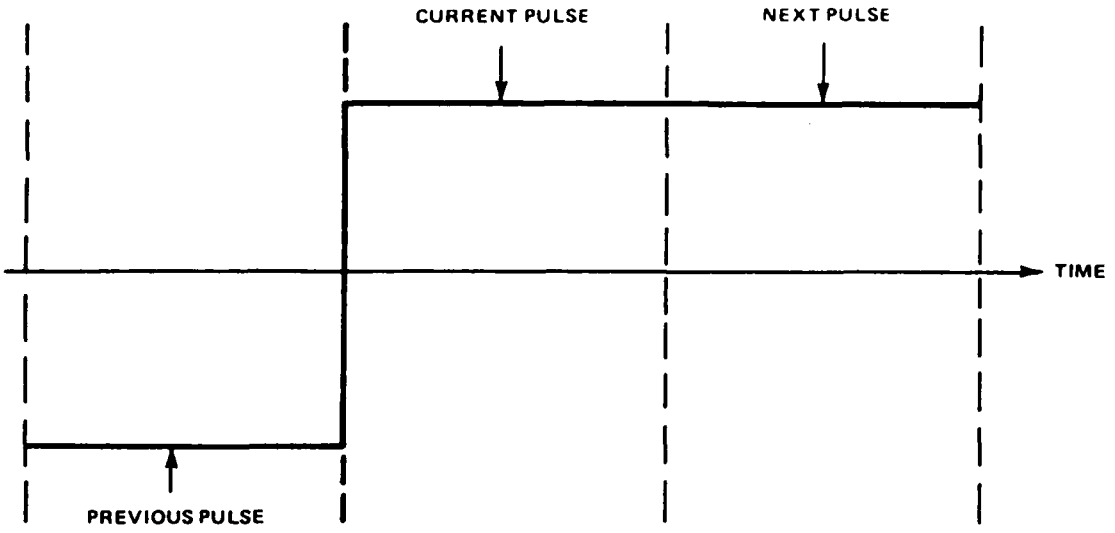

(a) NO INTERSYMBOL INTERFERENCE

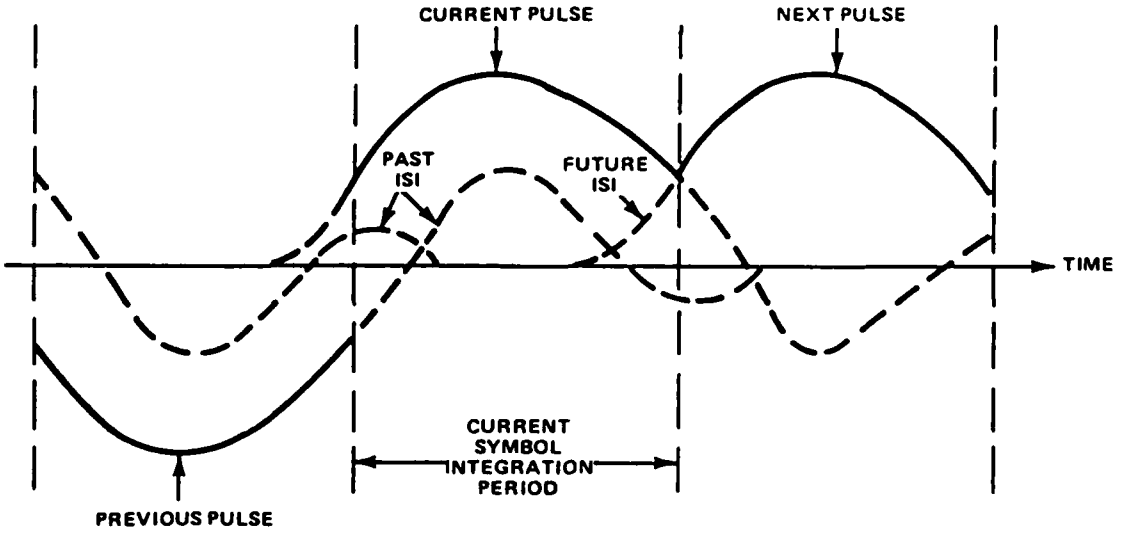

(b) INTERSYMBOL INTERFERENCE

Figure 2-2 Received Symbol Waveforms

2.2 SIMULATION MODELS

An equivalent link block diagram which shows the simulated link model in more detail is given in Figure 2-3. The input data sequence used in this simulation was an extended (0 added) 128-bit pseudo-random noise (PN) sequence. The PN sequence was chosen for its relatively good statistical randomness properties and its length was chosen to be significantly longer than the delay spread, yet shorter than the decorrelation time of the fading channel. Two intersymbol interference channel models were used in this study: a fixed tap finite length tapped delay line (TDL) model and a time-varying frequency domain transfer function model using the CIRF code.

The AMLSE receiver consists of two major components: The Viterbi maximum likelihood sequence estimation algorithm and the adaptive channel impulse response estimating filter. The Viterbi algorithm uses the impulse response estimates from the channel estimator to determine the maximum likelihood transmitted sequence. This sequence is used to update the channel impulse response estimating filter and is also differentially decoded and used to compute the symbol error rate (SER) performance of the system. Another SER measurement shown in this analysis was obtained assuming an ideal carrier tracking phase-locked loop which perfectly tracks the phase of the signal delay component with the largest average delay spread energy. More detailed descriptions of some of the major simulation subsystems are given in the following subsections.

2.2.1 Fixed Tapped Delay Line Channel

The tapped delay line channel model shown in Figure 2-4 was used mainly for testing and debugging the simulation. It operates by essentially convolving the information sequence, c_k, (in the case ±1's),

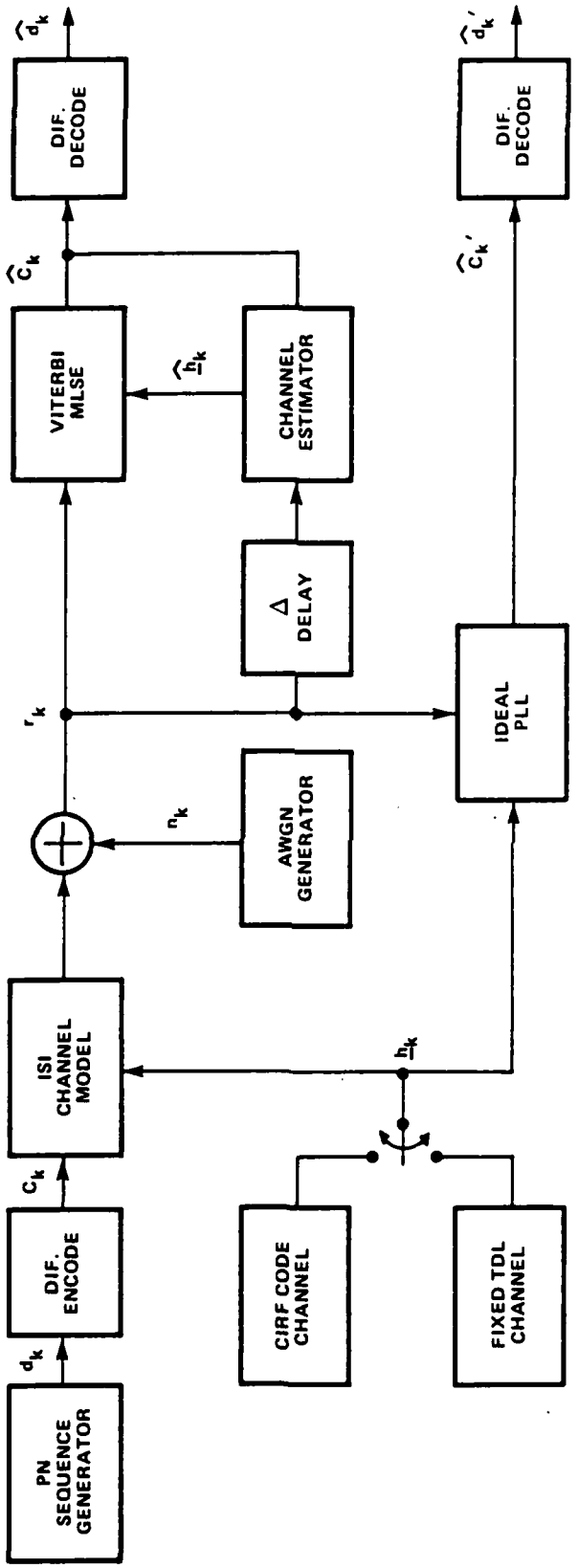

Figure 2-3 Block Diagram of Link Simulation Model

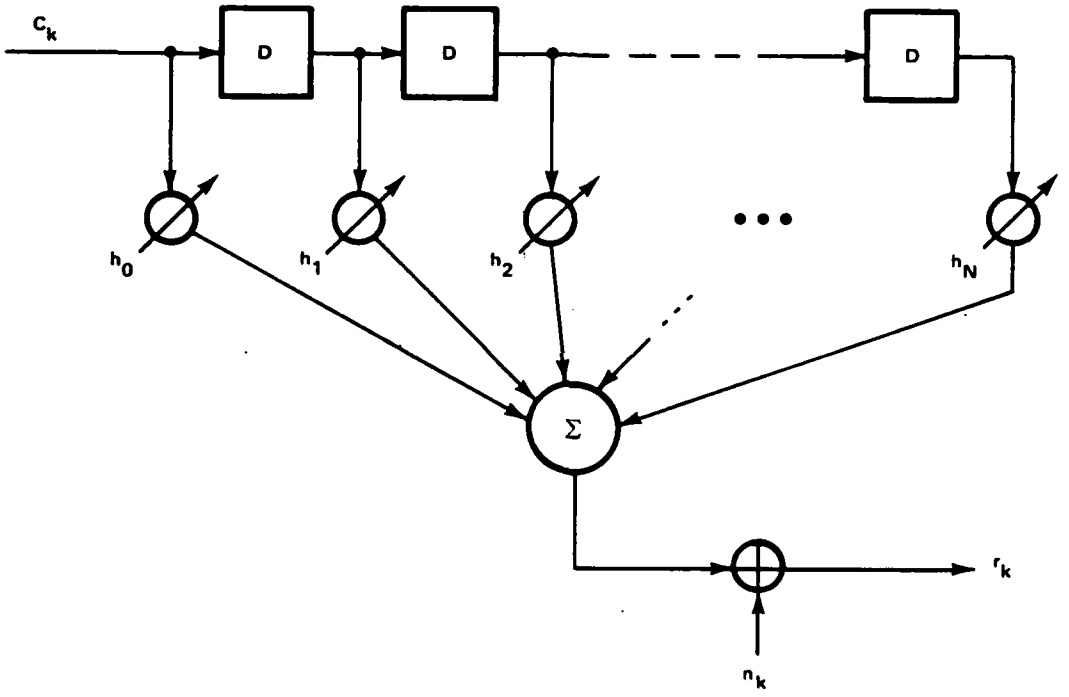

Figure 2-4 Fixed Tapped Delay Line Channel Model

with the channel impulse response represented by the complex channel tap gains h_0 to h_N as given by

$$r_k = \sum_{j=0}^{N} c_{k-j} h_j + n_k$$

Each succeeding tap gain is the complex impulse response at a delay of one additional information bit. Tap gain h_0 is therefore the impulse at zero delay.

This model was used to determine AMLSE noise performance and to evaluate losses due to estimation of the impulse response of the channel. This model has the advantages of being simple and also allows strict control over the impulse response and the number of taps having non-zero values. This was helpful in determining proper operation of the channel estimator.

2.2.2 CIRF Code Channel Model

The time varying channel was modeled using the CIRF Fortran program [1] which calculates time correlated random sample functions of the channel impulse response. The code simulates the channel impulse response according to the channel specification parameters. Two of the most important specifications are τ_o (decorrelation time) and f_o (frequency selective bandwidth). The program creates a two-dimensional complex matrix sample function in delay and time. At each time sample the one-dimensional function in delay is a channel impulse response similar to the set of taps in the tapped delay line channel model. The τ_o symbol is the average time in seconds for the autocorrelation of the channel impulse response as a function of time to reach a value of e^{-1}. The frequency selective bandwidth in Hertz of

the CIRF Code channel is given by $f_o \triangleq (2\pi\sigma_\tau)^{-1}$ where σ_τ is the rms value of the delay jitter dispersion. ISI is produced by random delays of the channel impulse response. The effect of this on the channel frequency response is to produce random phase and amplitude fluctuations or frequency selective fading. As ISI increases, the random phase and amplitude fluctuation decorrelation in frequency also increases. This produces a decrease of the selective bandwidth f_o.

This model was used to determine AMLSE performance in various ISI or FSF environments since it approximated an actual channel which varies with time.

2.2.3 Channel Estimator

The channel estimator is very similar to an adaptive linear equalizer. A diagram illustrating its operation is shown in Figure 2-5. Its purpose is to provide an estimate of the time-varying channel impulse response for the Viterbi algorithm to use in producing an estimate of the information actually sent. It does this by multiplying the estimated bit sequence (I_k), already calculated by the Viterbi (see Section 2.3 for detailed description) and stored in the tapped delay line, by the initial or previous estimate of the channel impulse response represented by the taps gains h_o to h_v. These products are summed to produce an estimate of the distorted received bit. This estimate is then subtracted from the actual received bit to form an error signal e_k. This value is reduced by the adaptation factor or coefficient, Δ, which controls the rate of adaptation and the stability of the estimator. This modified error value is multiplied by the estimated bit at each tap and this result is added to the prior tap gain. The new tap gains are used to form the next received bit estimate when the next estimated bit from the Viterbi is shifted into the tapped delay line. The set of tap gains are also

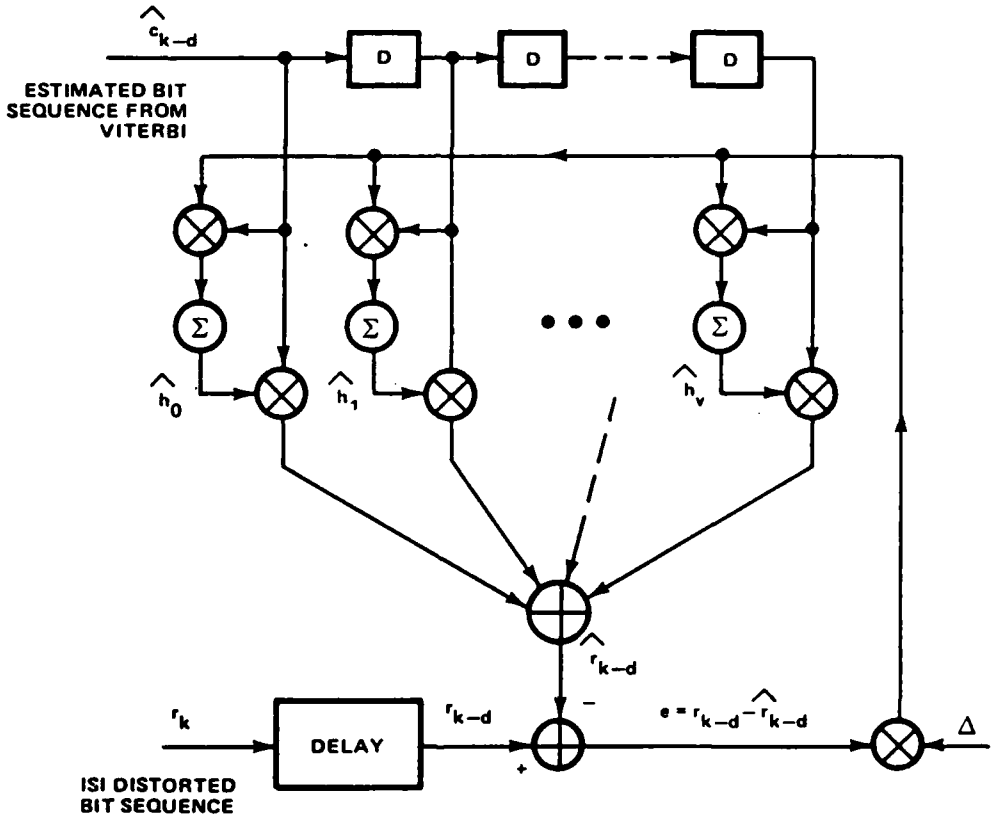

Figure 2-5 Channel Estimator

given to the Viterbi for its next computation. The tap gains (i.e., the channel impulse response estimate) are updated with new gains into the Viterbi every 128 bits. In general, the tap gains should be updated rapidly enough to accurately model the most rapid time-varying channel response.

2.2.4 Maximum Likelihood Sequence Estimation

Maximum likelihood sequence estimation was accomplished through the use of the Viterbi algorithm. A diagram for the illustrative sample case of a constraint length (K) of three is shown in Figure 2-6. In an actual simulation the Viterbi would have a constraint length equal to the number of taps desired to estimate the channel impulse response. It multiplies these tap estimates by all possible combinations of ±1's that could exist within the constraint length of the Viterbi. Each of these possible distortion combination products is then summed and this sum is subtracted from received value. The complex envelope of each of the differences is used as the branch metric.

These values are used by the Viterbi to determine the most likely sequence of bits within its memory. It was found that the memory length should be at least 4 to 5 times the constraint length, K.

The simulation model of the Viterbi was made to use a memory of up to 31 bits. About 20 bits memory were used for noise simulations and the full 31 bits for ISI simulations.

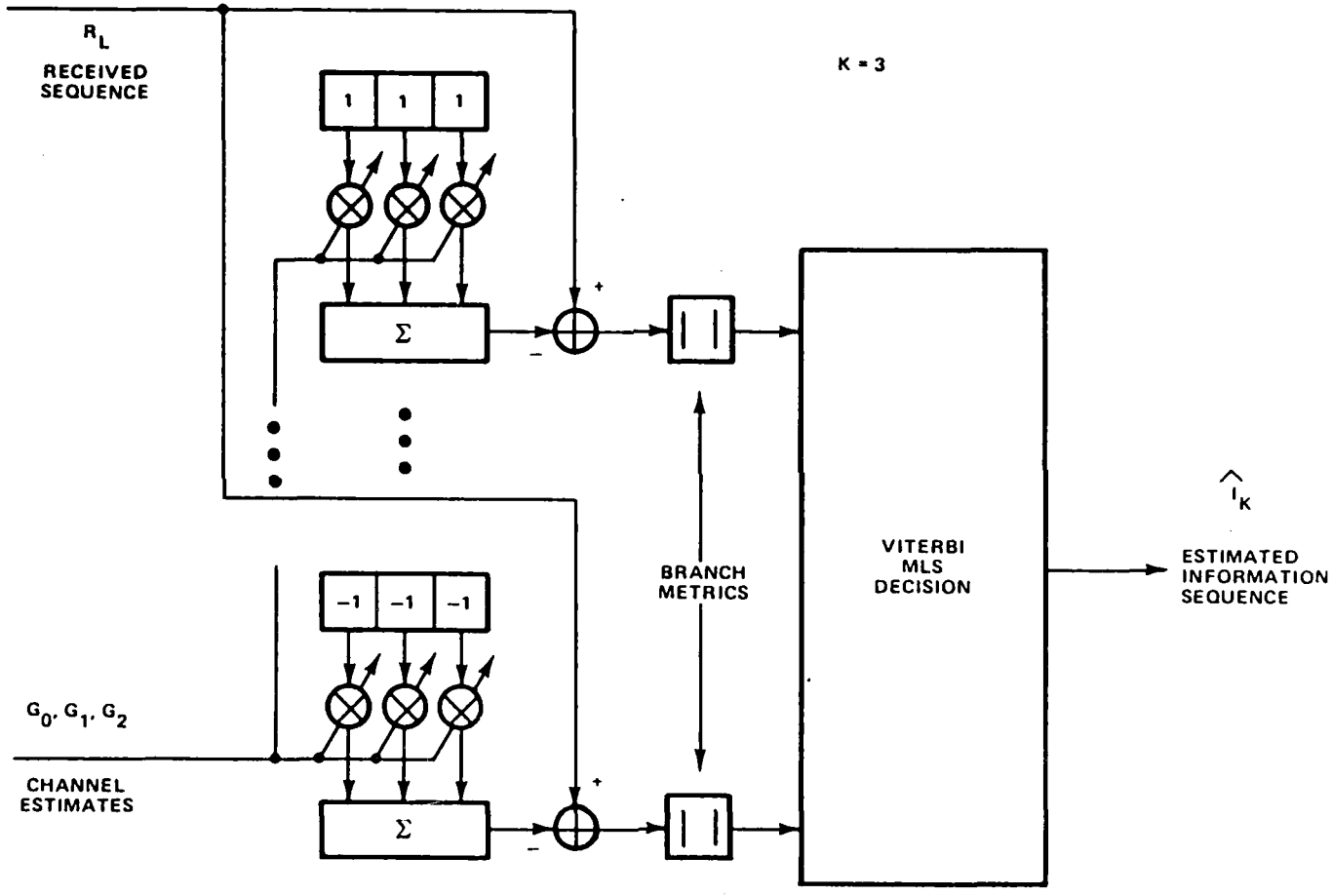

Figure 2-6 Viterbi Channel Decoder Simulation Program

SECTION 3

COMPUTER SIMULATION RESULTS

Several assumptions were applied to the simulations which produced the results contained in this section.

1) It was assumed the channel impulse response would change slowly as a function of time. For this reason the Viterbi was updated with new tap gains every 128 bits.

2) Each bit into the Viterbi decoder or channel estimator was assumed to be the output of an integrate and dump filter sampled once per bit.

3) Performance comparisons were based on symbol error rate (SER) comparisons.

4) The first four sequences or 512 bits were not included in the SER performance results to allow the receiver to reach an approximate steady state condition.

3.1 AMLSE PERFORMANCE IN AWGN ALONE

Five-tap AMLSE performance is compared to conventional CPSK performance in additive white Gaussian noise in Figure 3-1. The method of comparison is based on SER versus energy per symbol-to-noise density ratio (E_s/N_o). This comparison shows the loss due to the noise in the five taps. The channel estimator misadjusts the estimated impulse response away from the true response by interpreting the noise as ISI. This misadjustment noise produces some additional errors and a slight loss in performance (~½dB). It should be noted that a

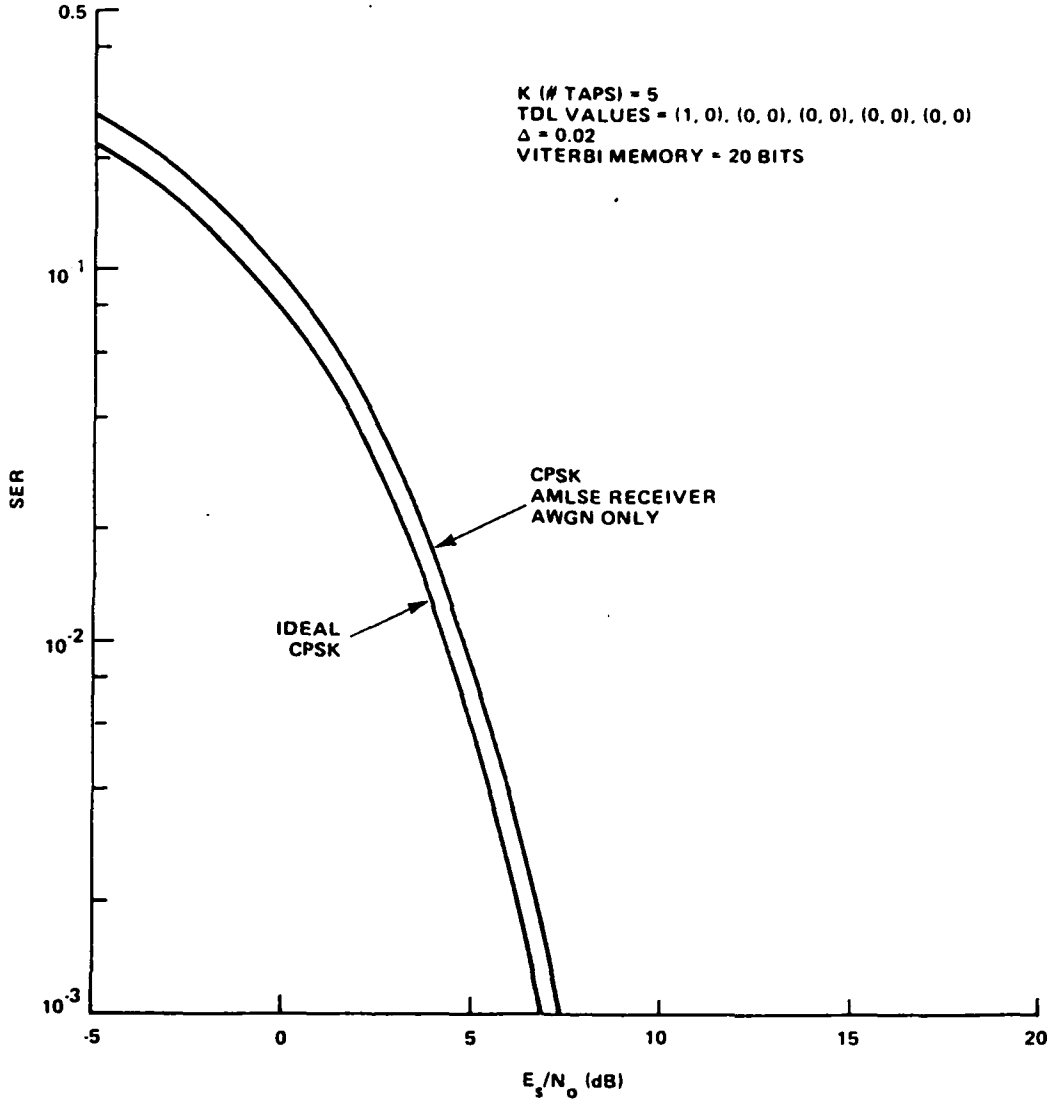

Figure 3-1 AMLSE and Ideal CPSK Performance in AWGN Alone

simulation using only two taps produced a curve almost indistinguishable from ideal CPSK.

It was found that for certain noise seeds the AMLSE receiver simulator using CPSK demodulation would produce symbol error rates near 0.5. It was determined that the channel estimator-Viterbi loop could reach a stable lock point when the estimated channel impulse response was opposite in sign to the actual response and the estimated information sequence from the Viterbi was also reserved in sign. When CPSK was used in these cases a SER approaching 0.5 could result. For this reason DECPSK (differentially encoded CPSK) was used for the remainder of the results. Figure 3-2 shows a comparison of SER performance for both conventional DECPSK and AMLSE using DECPSK demodulation added.

3.2 EQUALIZATION FOR FIXED CHANNEL AND AWGN

3.2.1 AMLSE Simulations

As an initial test case, the tapped delay line (TDL) channel model was used for the simulation of the AMLSE. The number of taps and their values were fixed known values. By taking advantage of these properties the effectiveness of the channel estimator could be determined. Figure 3-3 illustrates the loss that can be expected from the estimator due to imperfect estimates of the tap gains. In the lower curve the Viterbi was given the true channel tap gains of the TDL channel model and the channel estimator adaptation constant, Δ, was given a zero value. When the simulation was repeated with Δ equal to 0.02 the loss was always less than 0.5dB for SER's less than 0.1. The curve at the top of the figure shows the receiver performance without adaptive maximum likelihood sequence estimation for the same TDL IDI sequences.

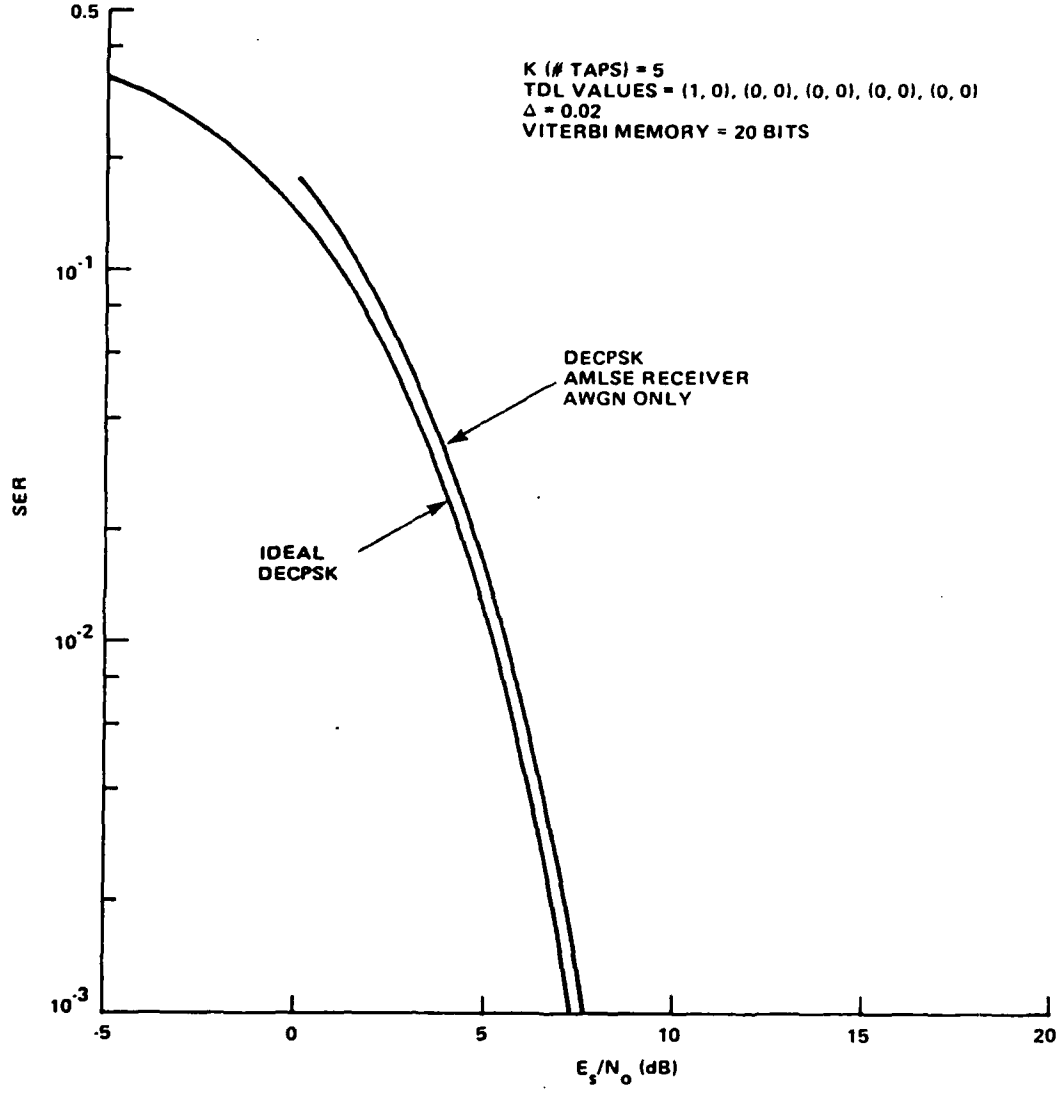

Figure 3-2 AMLSE and Ideal DECPSK Performance in AWGN Alone

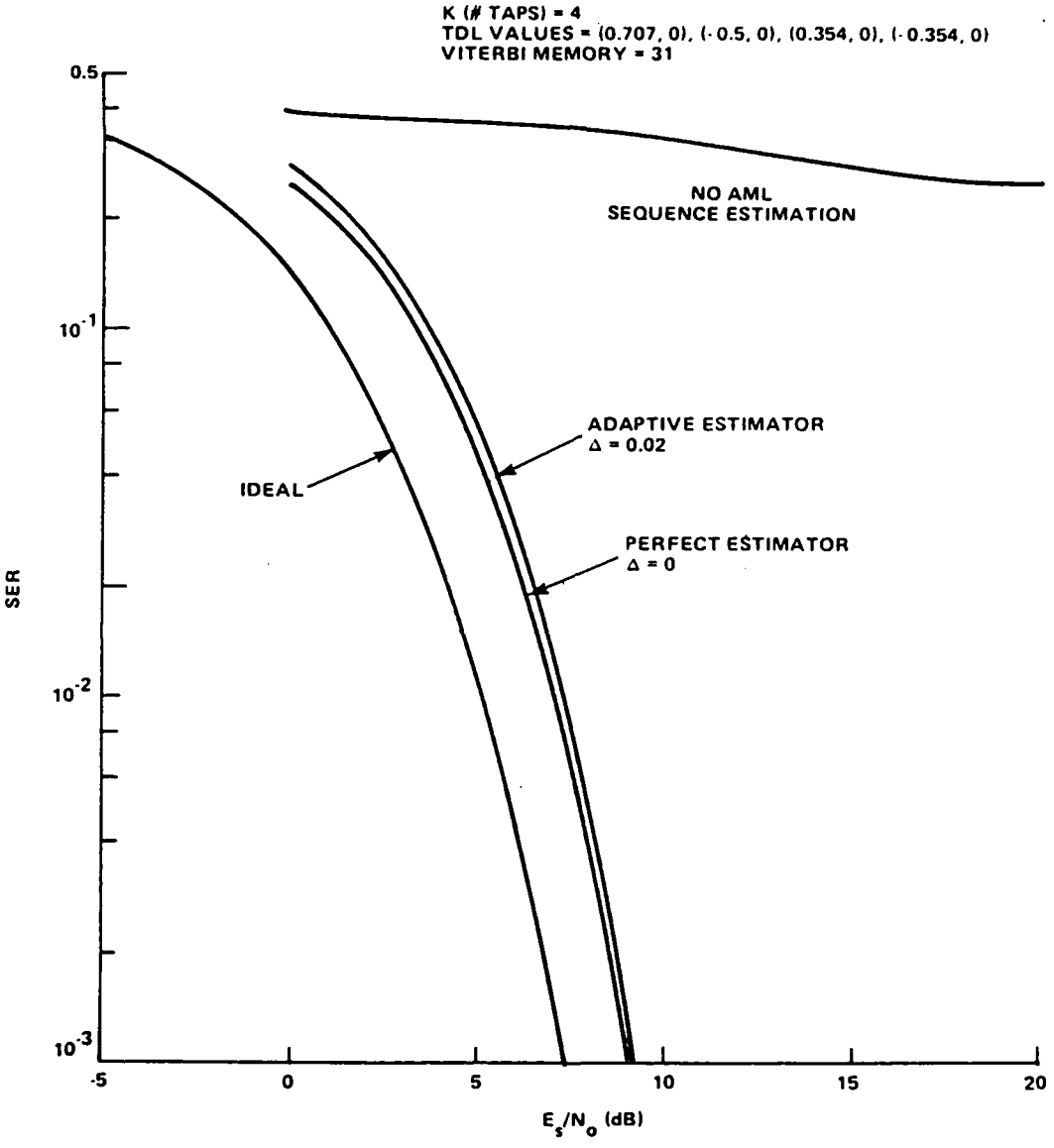

Figure 3-3 AMLSE Performance in AWGN With A Fixed TDL Channel Model

The 2dB difference between ideal DECPSK and the results from the TDL model is due to the form of the channel impulse response and the frequency of occurence of certain "bad" data subsequences. This is explained by Magee [8] and Forney [9]. They show that the upper and lower bounds on the symbol probability of error are dependent on the channel response. Thus, if the channel changes then the expected steady-state SER will also change.

3.2.2 Comparison of AMLSE with Decision Feedback Equalization (DFE) for a Fixed Channel

In order to estimate the performance improvements afforded by the AMLSE processing over the DFE processing, a number of fixed tap delay channels were tested for both techniques. The channel responses shown in Figures 3-4 and 3-5 are typical of telephone channel responses although they could equally well represent a sample function of a random time-varying selective channel.

A DFE processor block diagram for binary antipodal signalling is shown in Figure 3-6. The feedforward section (with taps G_o, G_1,..G_{M_f}) effectively "equalizes" the effects of the future symbols while the feedback section (with taps G_1, G_2, ... G_{M_b}) removes (i.e., subtracts) the effects of the prior symbols or bits based on the decisions made in the sign circuit shown in the figure.

The performance results of the DFE for channels B and C are shown in Figure 3-7 for a 15 forward tap and 15 feedback tap DFE configuration and differential demodulation with no coding. The simulation results (triangle in figures) were also compared to the simulations (solid lines in figures) presented in Reference [7] to verify program/algorithm correctness. Note that the performance varies widely and is worse for channels tending toward large "spread" and nearly equal components.

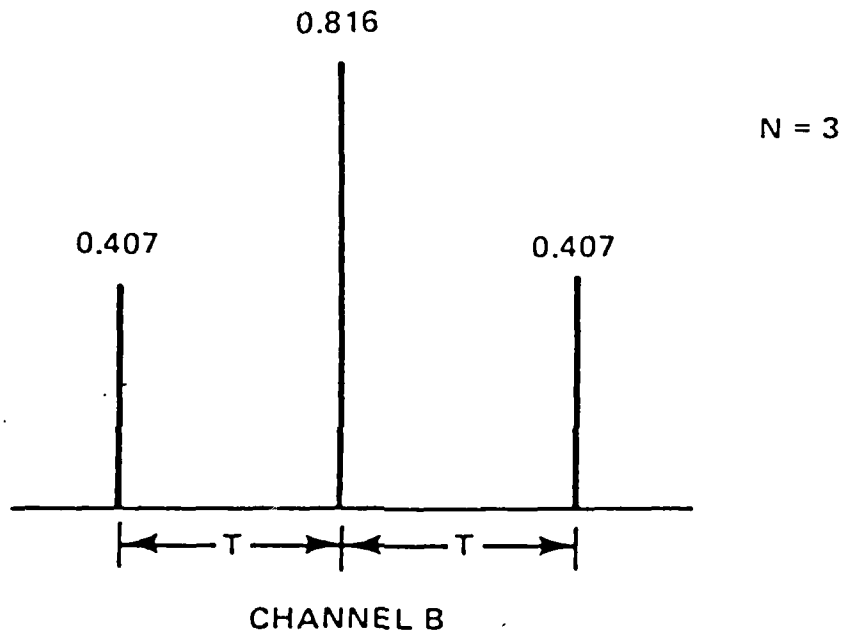

Figure 3-4 Fixed Channel Impulse Response B

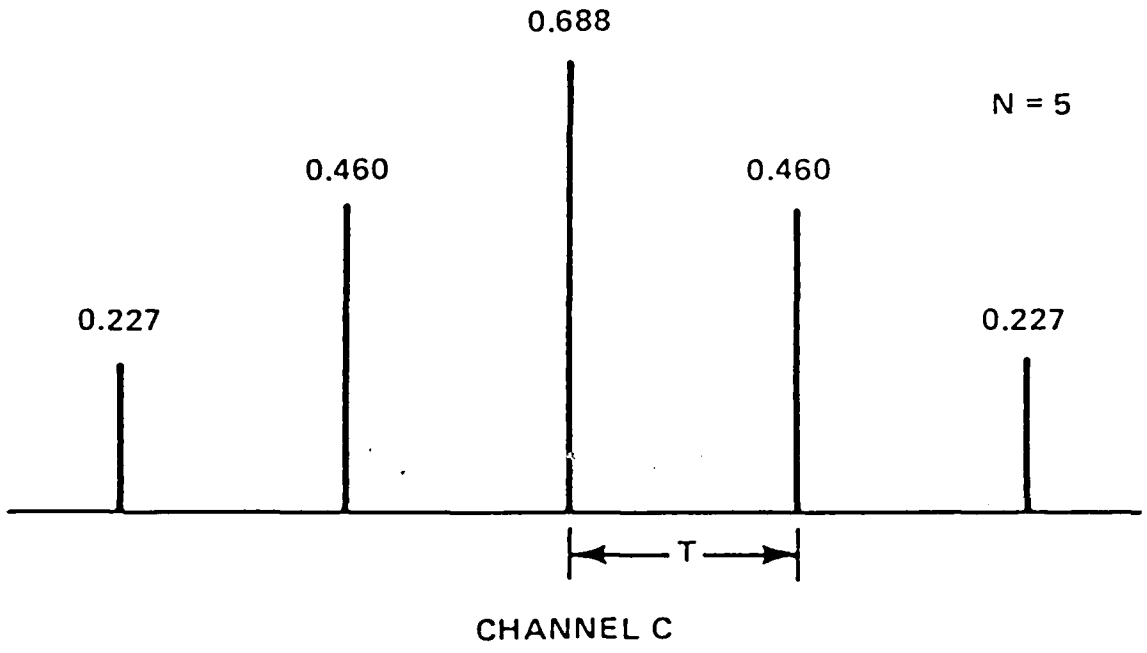

Figure 3-5 Fixed Channel Impulse Response C

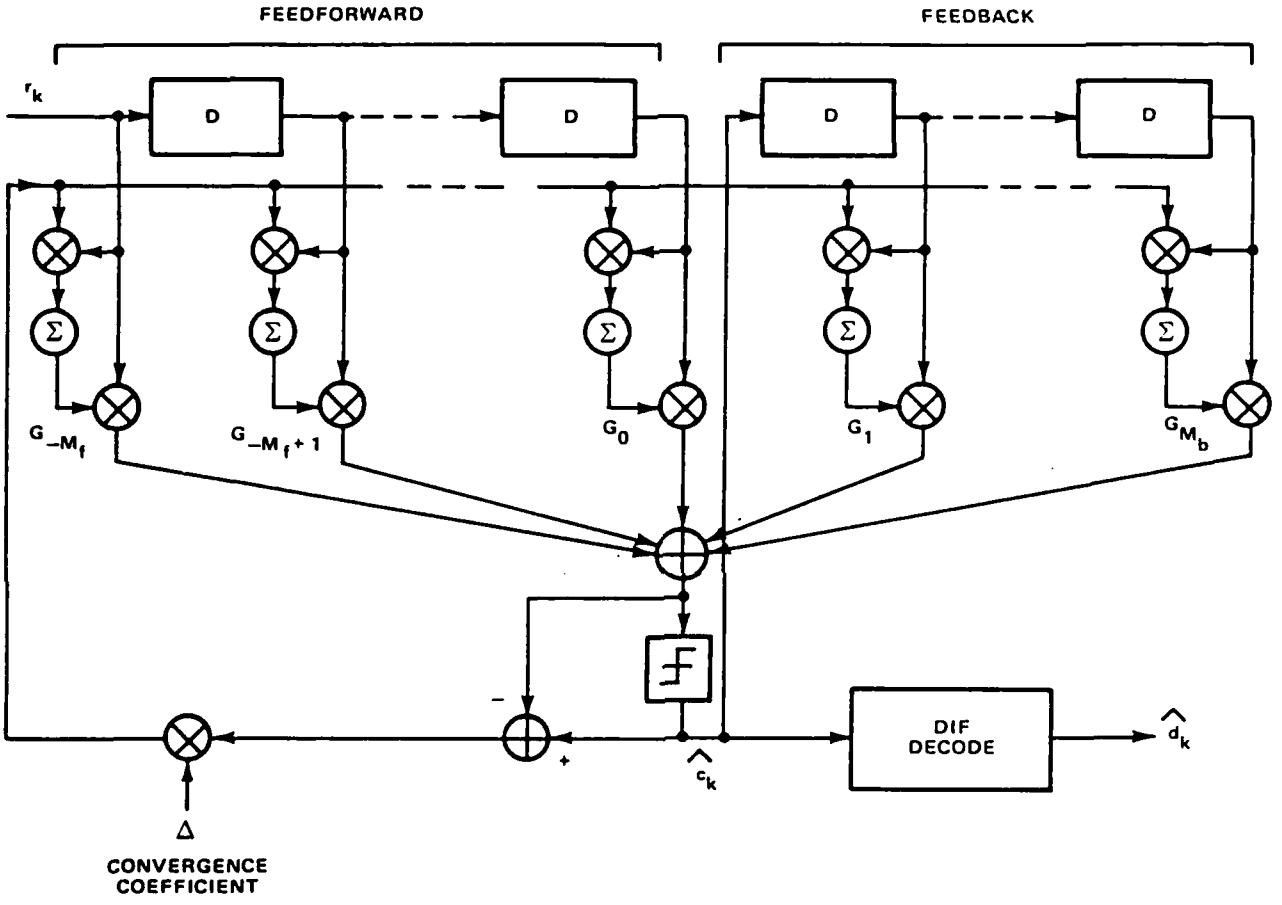

Figure 3-6 Decision Feedback Equalizer

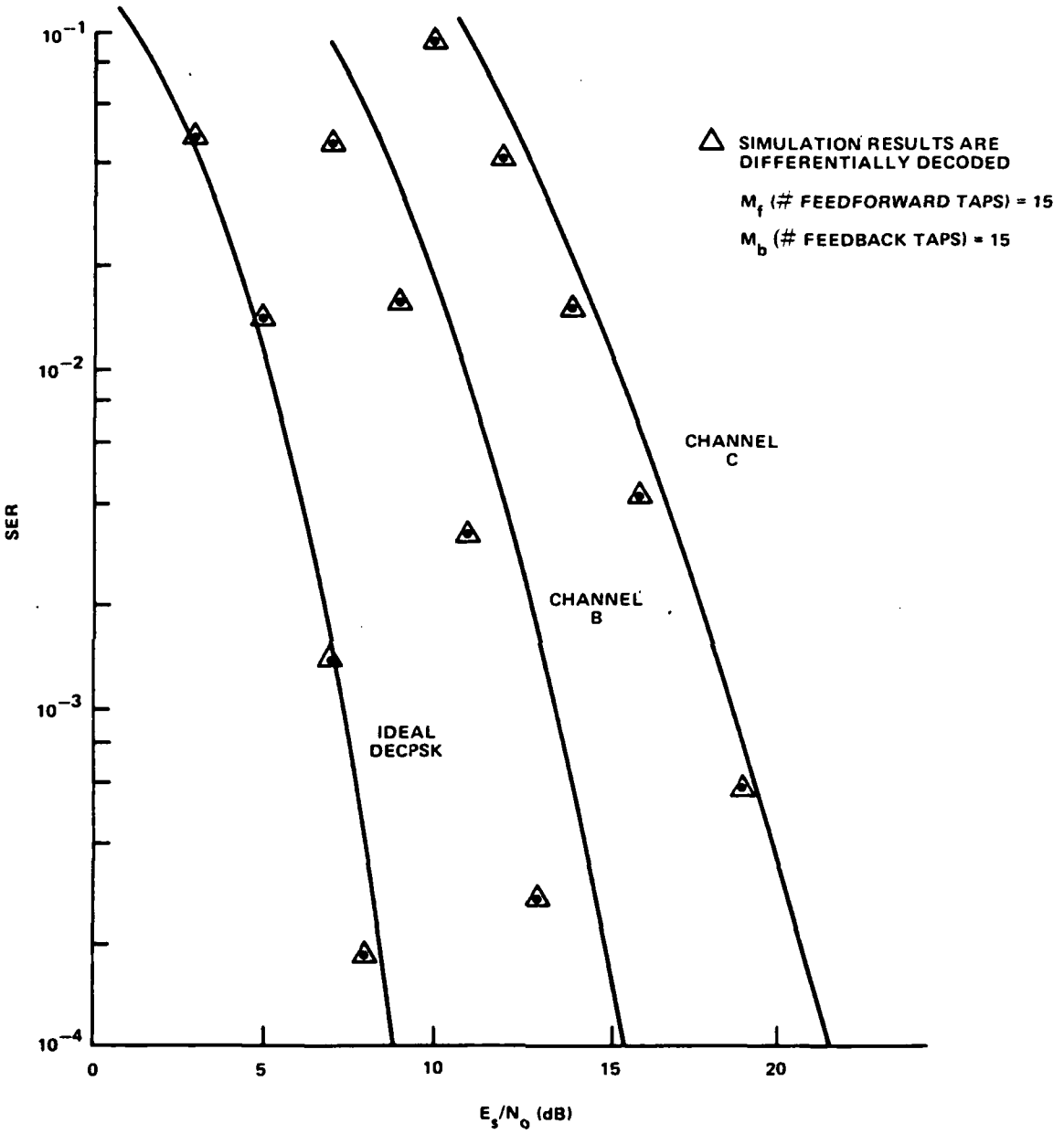

Figure 3-7 Performance of DFE for Fixed Channels

This phenomenon occurs for a "flat" response channel simply because these channels will tend to have more bandwidth (due to sharp drop offs) as well as spectral nulls or zeroes which make spectral inversion extremely difficult (i.e., a perfect null implies infinite response or "noise" when inverted). Therefore, it follows that when the time-varying (CIRF) selective channel yields a shape such as in Channel C, the equalization process will incur a high error rate ($\sim$10% error rate for E_s/N_o = 10 dB as shown in the figure).

The AMLSE receiver (channel estimator convergence parameter Δ = 0.01) yielded the significantly better results shown in Figure 3-8. The reason is that the AMLSE is an optimal sequence matched filter and therefore minimizes the probability of sequence error, whereas the decision feedback filter merely minimizes the mean square error between the received symbol and the estimate on a symbol-by-symbol basis. It is the optimal sequence estimating property that allows the AMLSE processing to "correct" symbol errors inside the sequence (that the DFE would have made) much like the Viterbi error correction decoder corrects bit errors over several constraint lengths when decoding convolutional codes.

Further evidence of the superiority of AMLSE processing over DFE will be shown for a time-varying selective channel in Section 3.5.

3.3 EQUALIZATION FOR A CIRF TIME-VARYING FREQUENCY-SELECTIVE CHANNEL

Equalization techniques, such as Decision Feedback, evaluated for fixed channels have been applied very successfully in the past to slowly-varying telephone channels, however, their effectiveness for very rapidly varying severely-dispersive (selective) channels is not well-known except for some preliminary work in mildly selective troposcatter channels [12].

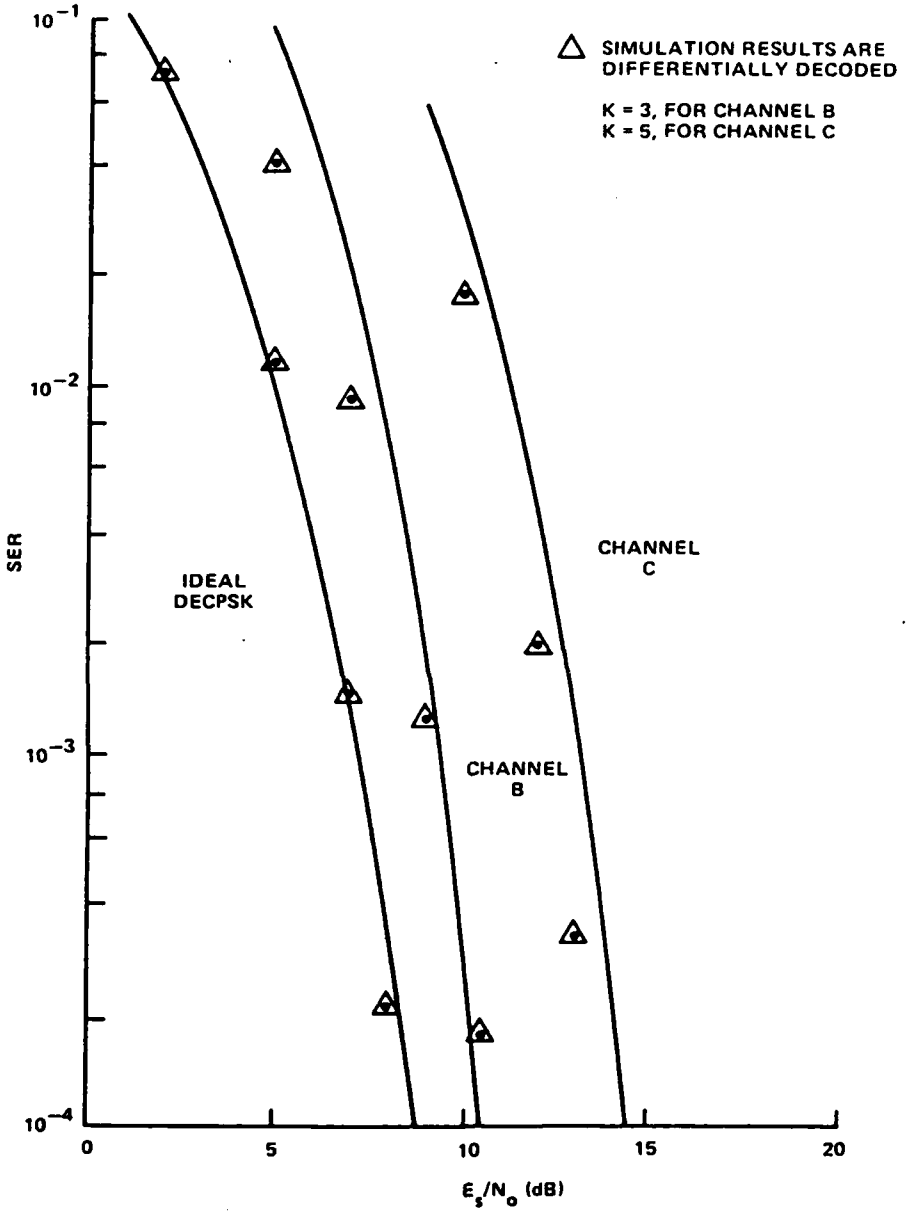

Figure 3-8 Performance of AMLSE for Fixed Channels

In this section, the performance of a number of refined versions of AMLSE are presented for the time-varying CIRF dispersive channel as a function of the frequency selective bandwidth. The decorrelation time evaluated was chosen to be roughly 1000 bits to simulate the effects of a moderately rapid time-varying channel. Previous results [11] have used a ratio of approximately 10,000. The decorrelation time is defined as τ_o, which is the e^{-1} point of the fading temporal covariance function for a tone at the carrier frequency. It should be noted that the fluctuation period of any delay component (of the channel impulse response) may not be equal to τ_o, and, in fact, the fluctuations are generally much more rapid for longer delay components (see Figure 3-11). This channel characteristic of different parts of the channel impulse response varying at different rates further compounds the problem of proper equalization and channel estimation.

The following subsections will present the results of various trade studies considering the false lock phenomena, the determination of proper channel estimator convergence constants, a comparison of AMLSE (with DFE equalization also) and AMLSE only vs. DFE equalization for various SNR's and channel coherence bandwidths. Due to both a false lock phenomena (to be discussed in Section 3.3.1) and a desire to evaluate various systems independent of bit sync tracking performance, the results presented in this section assume ideal data is fed back to both the channel estimator for the AMLSE and to the feedback delay line for the DFE.

3.3.1 False Lock Phenomenon

This section will focus on the results of an investigation of the false lock phenomenon (multiple stable lock points) of the adaptive maximum liklihood sequence estimation (AMLSE) operating in a delay spread CIRF code channel. This phenomenon is characterized by the condition that the channel estimator produces a shifted (n bit offset estimate of the true channel response.

In general, faster fading channels make it more difficult for the channel estimator to track the faster variations of the channel. The poor channel estimates result in a greater number of errors from the Viterbi which in turn further degrade the channel estimates through the AMLSE demodulated data that is fed back to the channel estimator. This cycle ultimately causes the channel estimator to temporarily lose track of the actual channel until a significant portion of the delay spread channel power clusters together at a single delay value. This clustering would temporarily provide a higher SNR which would enable the channel estimator and sequence estimator to relock, however, the estimate would sometimes be shifted by a bit or two in delay. Note that if both the sequence and the channel estimator are offset by the same amount, the AMLSE processor will be in another stable lock state since the error signal in the channel estimator is essentially unchanged and the shifted distortion combination sums of sequence estimator will be aligned with the shifted Viterbi memory state. Some of these effects are shown in the following figures.

Figure 3-9 is a plot which shows the envelope of the channel estimate of the channel estimator of the AMLSE for a CIRF code simulated frequency selective fading channel. The time axis goes into the paper and each trace represents a noiseless envelope of the channel impulse

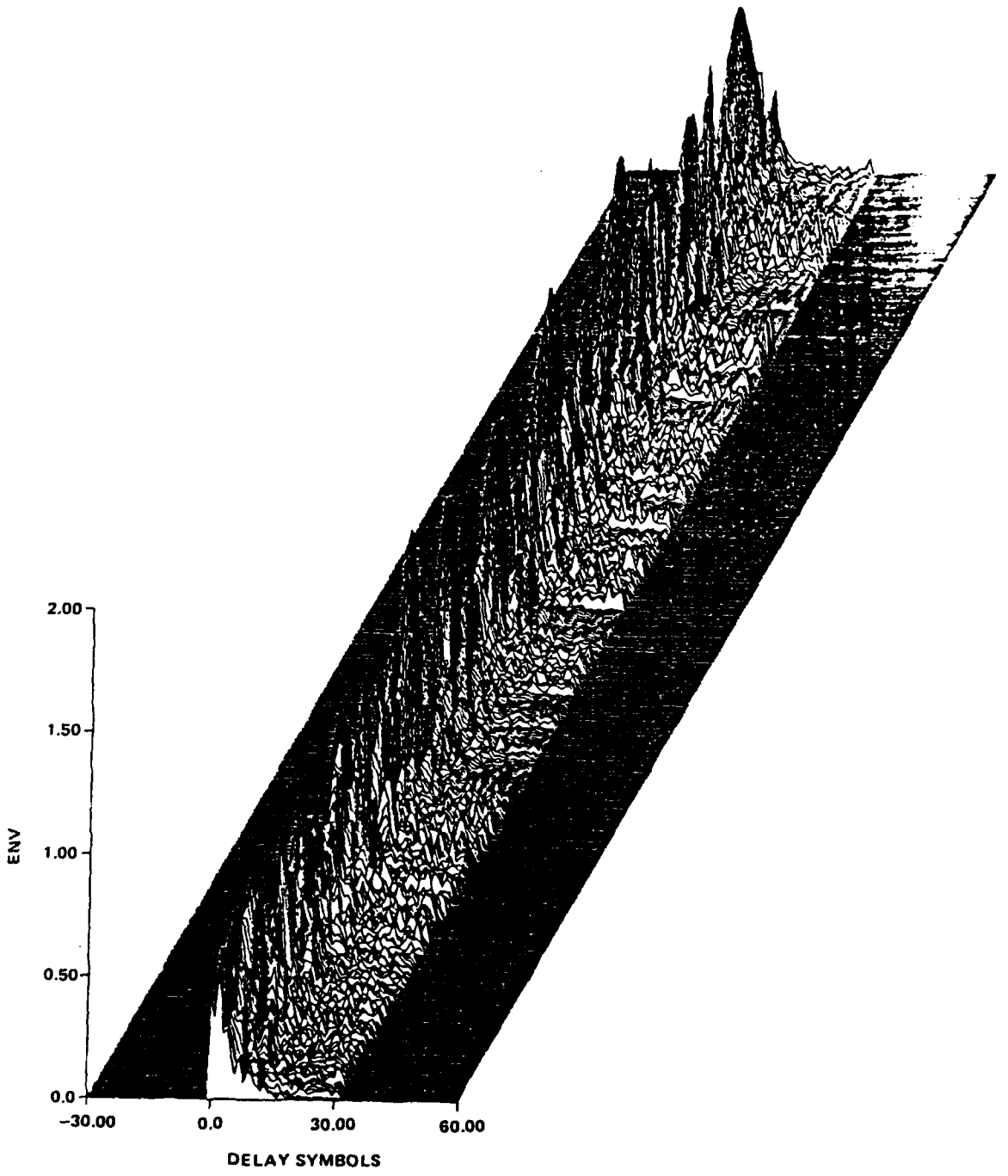

Figure 3-9 Estimated Channel Impulse Response as a Function of Time

response at an interval of one tenth of the channel τ_o. It can be seen that there are portions of the estimated channel impulse response where abrupt envelope changes occur at larger delays. A closer inspection will show that these transitions occur after simultaneous fades at all delay positions of the channel impulse response and continue until the next simultaneous fade occurs. The fades frequently cause the channel estimator to lose lock and produce noisy spikes at large delays shown in Figure 3-9.

Figure 3-10 is a similar plot of the noiseless envelope of the channel estimate when the channel estimator is given perfect information sequence which we call Ideal Information Estimation (IIE). When Figure 3-10 is compared to the actual channel in Figure 3-11 it can be seen that the channel estimator can produce accurate estimates of the true channel at all delays with sufficient signal energy if the Viterbi's decisions are correct.

One of the main causes of poor channel estimation in Figure 3-9 is the mismatch between the length of the actual channel and the constraint length (K) of the Viterbi decoder (i.e., K is less than the channel spread). The unmodeled channel response appears as an additional noise degradation at the demodulator. A possible solution to this problem is discussed in Lee [10] who proposed a receiver structure similar to Figure 3-12 which uses the feedback portion of a Decision Feedback Equalizer (DFE) as a prefilter to remove the effects of delay components beyond the sequence estimator constraint length to in effect provide the Viterbi sequence estimator with a signal distorted by a shorter finite duration impulse response channel. It is believed that this will directly improve the symbol error rate out of the Viterbi. In a subsequent section, this new technique using prefilter aiding via tentative Viterbi decoder decisions will be implemented and discussed.

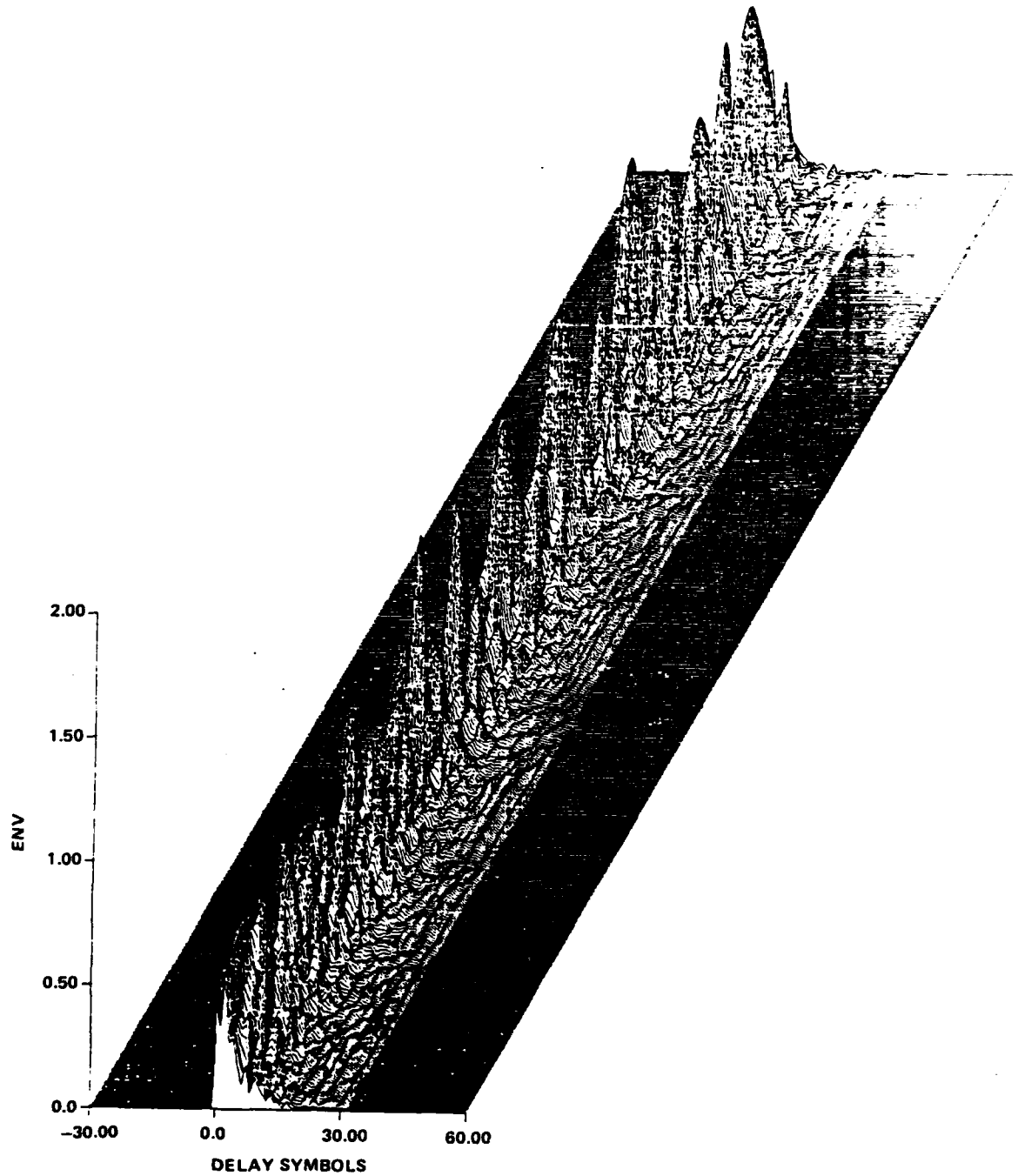

Figure 3-10 Channel Impulse Response Estimate Using Ideal Information Estimation (IIE)

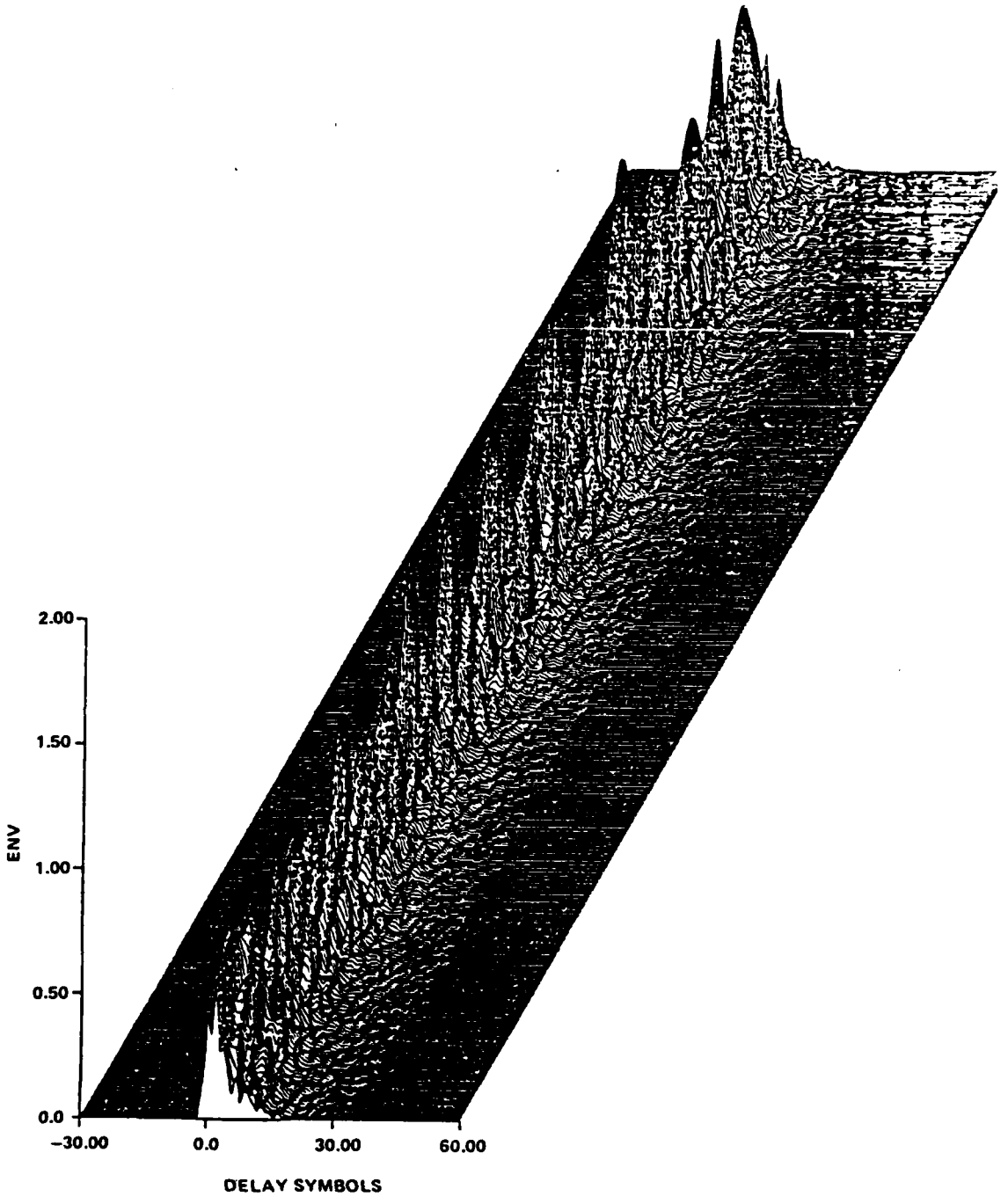

Figure 3-11 True Channel Response

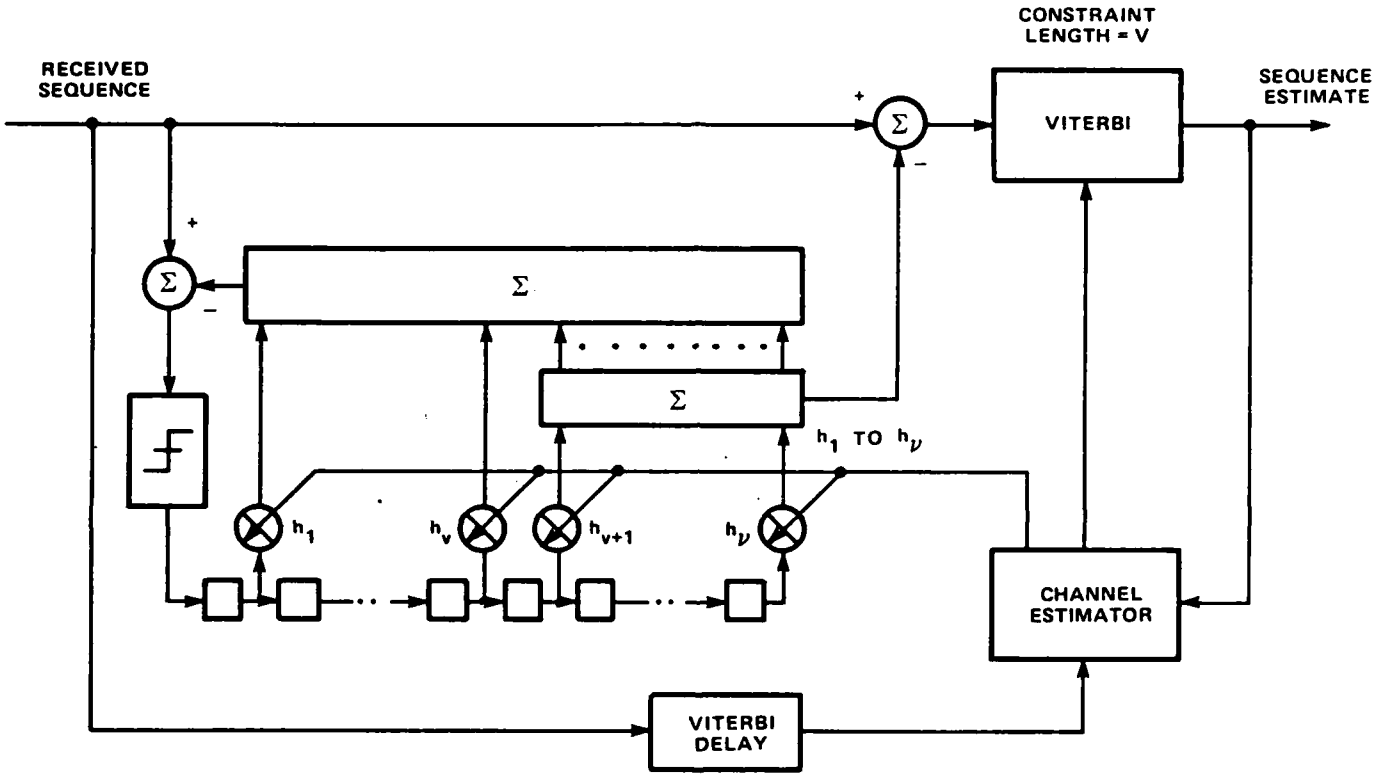

Figure 3-12 Maximum Likelihood Sequence Estimation with Decision Feedback Equalization Pre-Filtering

3.3.2 Adaptivity Coefficient Optimization

A significant effort was made to optimize Δ(the adaptation constant) for each value of f_o, K, and number of taps since one can deduce a robust Δ value from the family of curves. The result of this analysis is shown in Figures 3-13, 3-14, and 3-15 for K=4, 6, and 8 respectively (for a fixed $R_D\tau_o$= 1,000). These curves show the optimal Δ(determined by the minimum SER for a particular R_D/f_o) decreases as R_D/f_o increases for a fixed K and increases as K increases for a fixed R_D/f_o. For the cases considered, the optimal Δ was always below 0.03 for R_D/τ_o=1000. For the remainder of the results a value of 0.02 was used in the simulations. The Δ can be scaled directly with the $R_D\tau_o$ ratio, i.e., 0.002 would be chosen for a $R_D\tau_o$=100 simulation.

The simulation results were obtained by giving the channel estimator the perfect information sequence (IIE). This eliminated channel estimate dependence on the SER of the Viterbi and thereby the possibility of bit slips. As a result, any bit errors that occurred were only due to the inadequate number of taps used to represent the channel.

Using the inforamtion from Figures 3-13, 3-14, and 3-15 at a Δ of .02 another graph was constructed to show AMLSE performance as a function of K, the number of taps estimating the channel impulse response. These results are shown along with the results from ideal channel estimation simulations in Figure 3-16. Recall that ideal information estimation implies that the channel estimator was given the original information sequence as if the Viterbi were operating perfectly as explained in the previous paragraph. Ideal channel estimation (ICE) means that the Viterbi was given the first K values of the actual impulse response as if the channel estimator were operating perfectly. A comparison of the dashed and solid lines for each R_D/f_o shows the performance loss due to imperfect channel estimates given to the Viterbi. This loss increases as K increases for a fixed R_D/f_o.

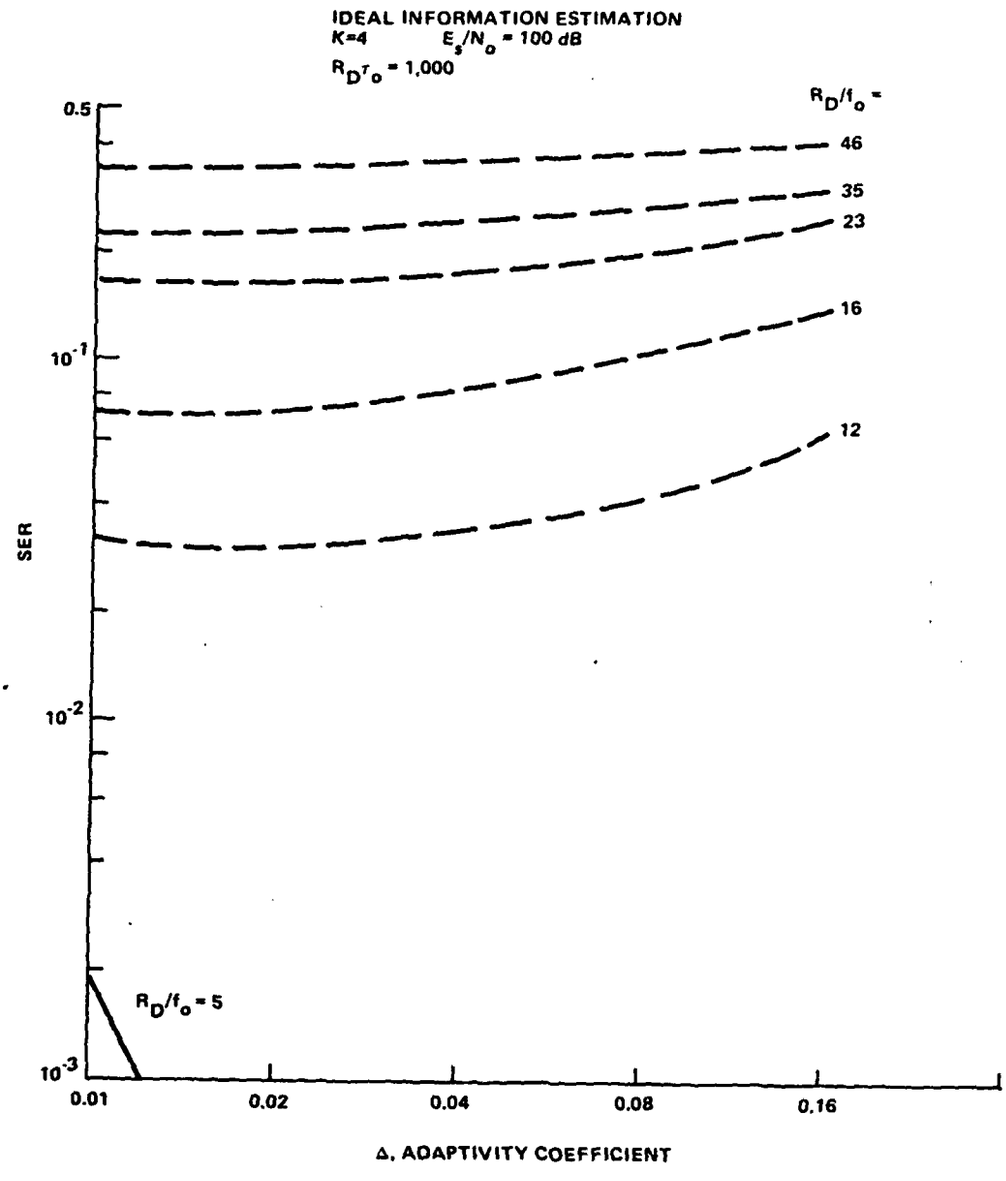

Figure 3-13 Performance vs. Adaptivity Coefficient for K=4

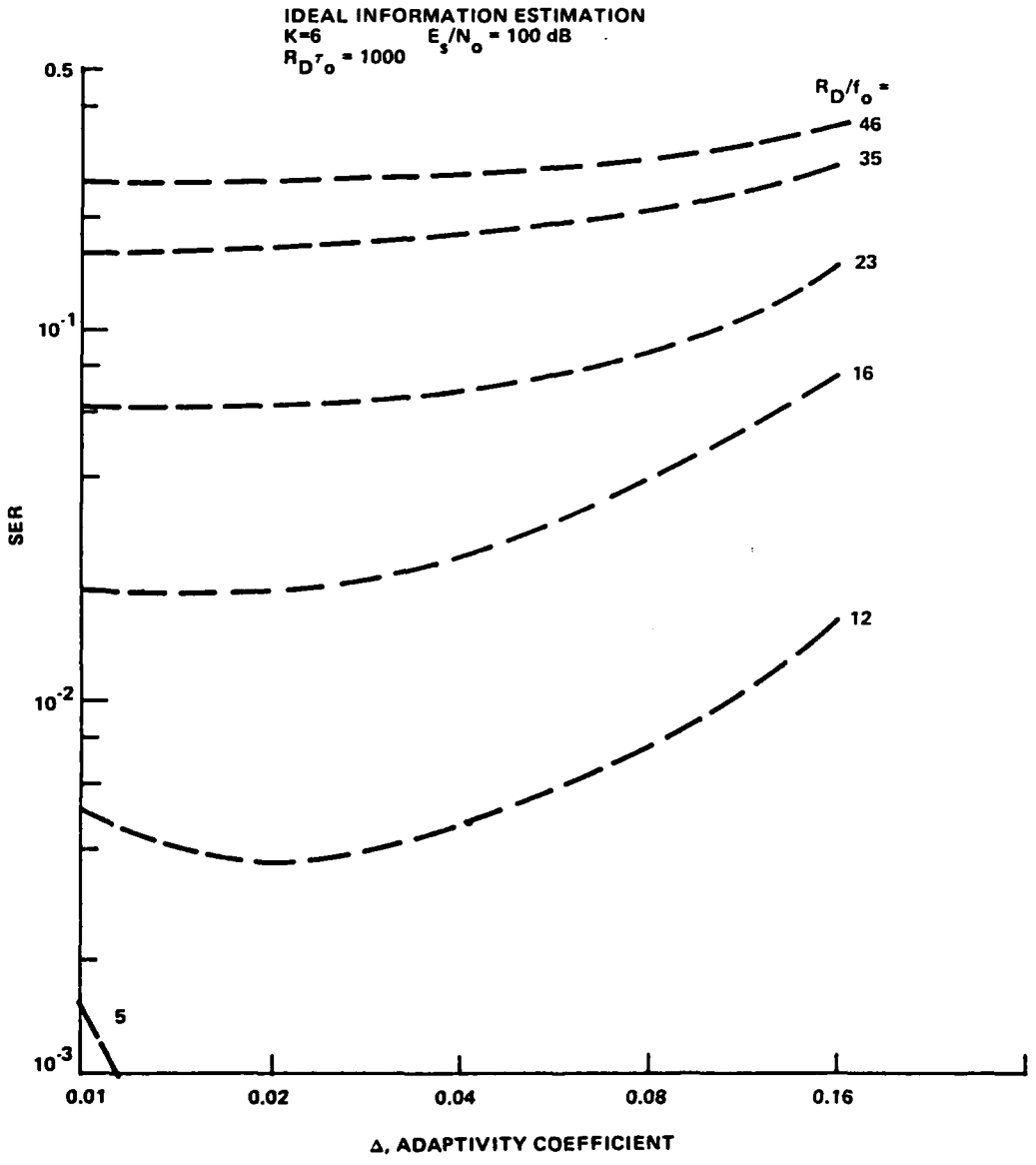

Figure 3-14 Performance vs. Adaptivity Coefficient, K=6

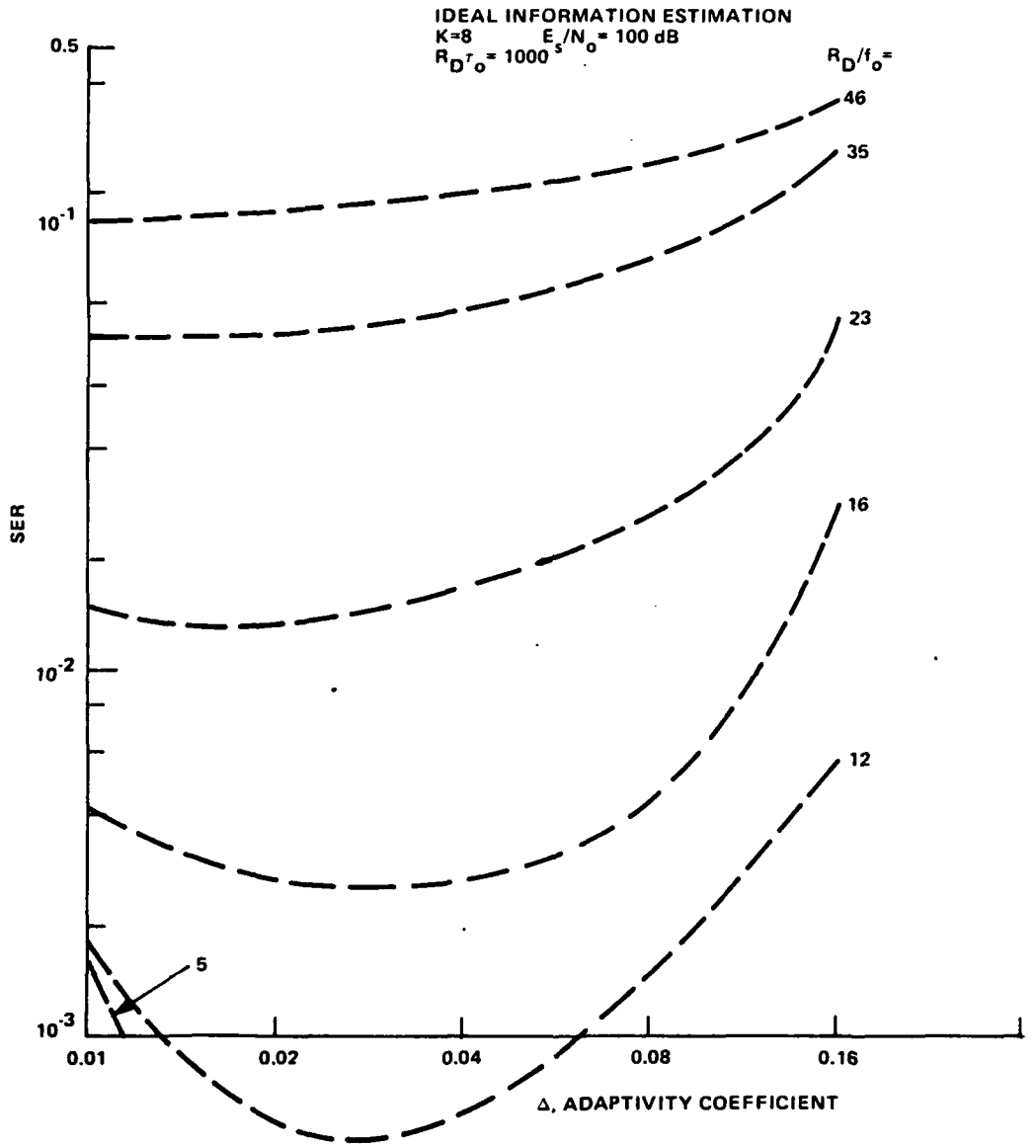

Figure 3-15 Performance vs. Adaptivity Coefficient, K=8

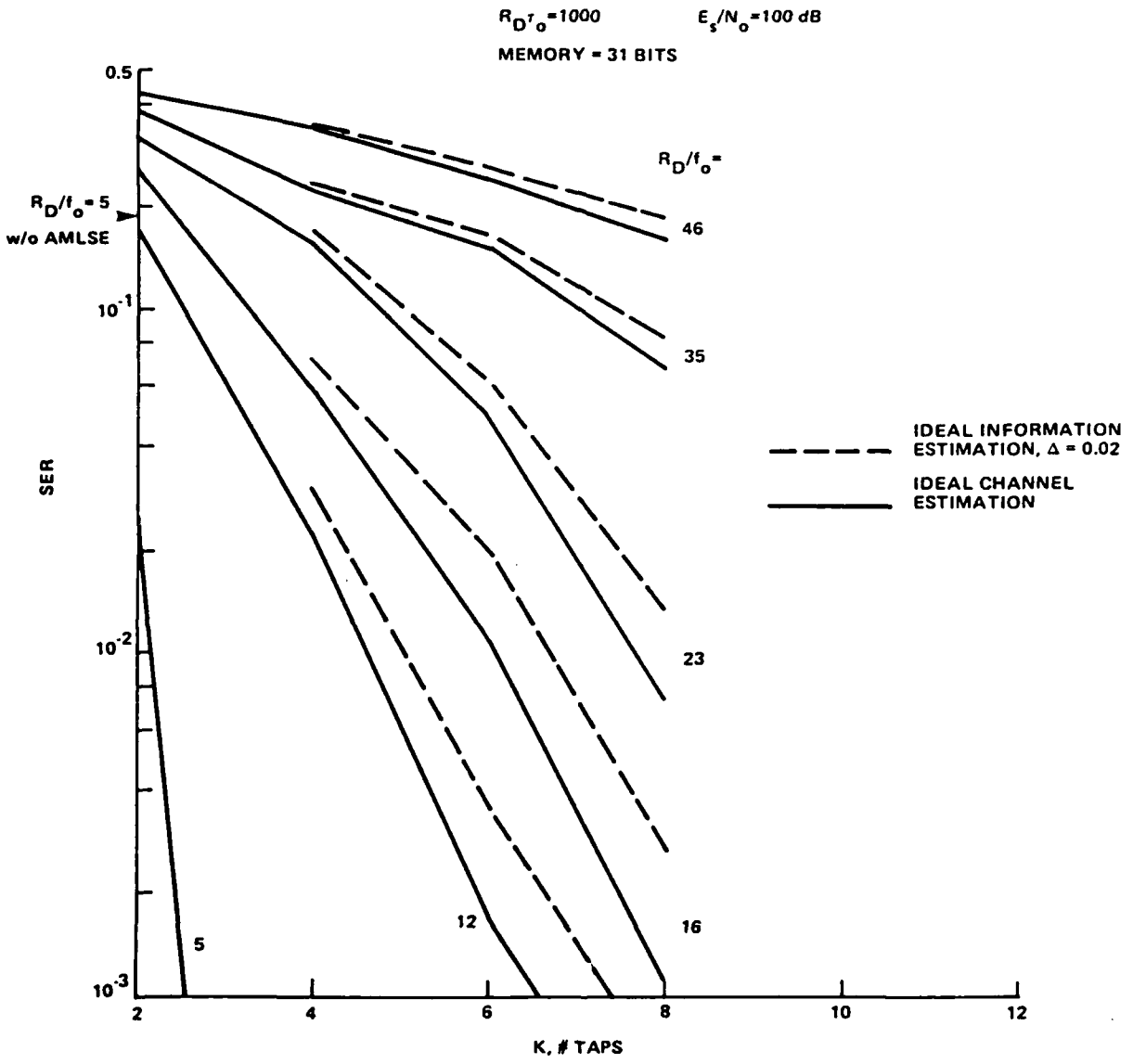

Figure 3-16 AMLSE Performance vs. R_D/f_o and K for Optimal Adaptivity Coefficient (Δ =0.02)

This graph also demonstrates the improvement in performance obtained as the number of taps estimating the channel impulse response is increased for a fixed R_D/f_o. An R_D/f_o below about 1 would be considered flat fading. An R_D/f_o of 5 would have little ISI since it is fairly close to flat fading while any R_D/f_o greater than 20 would be considered a severe ISI environment. The arrow at a SER of approximately 0.185 shows the receiver performance for an R_D/f_o of 5 without AMLSE capability for comparison (higher R_D/f_o values will result in worse performance).

3.4 AMLSE PERFORMANCE IN A TIME-VARYING DISPERSIVE (CIRF) CHANNEL

Performance curves for the AMLSE in a time-varying (CIRF) channel are shown in Figures 3-17, 3-18, and 3-19 for a K of 4, 6, and 8 respectively. It was expected that each curve would asymptote toward a SER of 0.5 at low SNR and asymptote at the appropriate SER as shown in Figure 3-16 at high SNR. These asymptotes correspond to the limiting effects of noise at low E_s/N_o and ISI at high E_s/N_o. The ISI asymptote is actually caused by the inadequate number of taps used to estimate the channel impulse response. The energy lost by using this finite number of taps acts as an extra noise component which is independent of E_s/N_o.

These graphs show an E_s/N_o greater than 20 dB would provide very little performance improvement, but an E_s/N_o less than about 12 dB would degrade performance substantially. The curves again demonstrate the degradation due to imperfect channel estimation.

3.5 AMLSE EQUALIZATION WITH DFE PRE-FILTER

A modified adaptive maximum likelihood sequence estimator which uses a form of decision feedback (AMLSE/DFE) to reduce the effect of mismatch between a long channel impulse response function and the shorter (run-time constrained) Viterbi estimator constraint length is analyzed in this section.

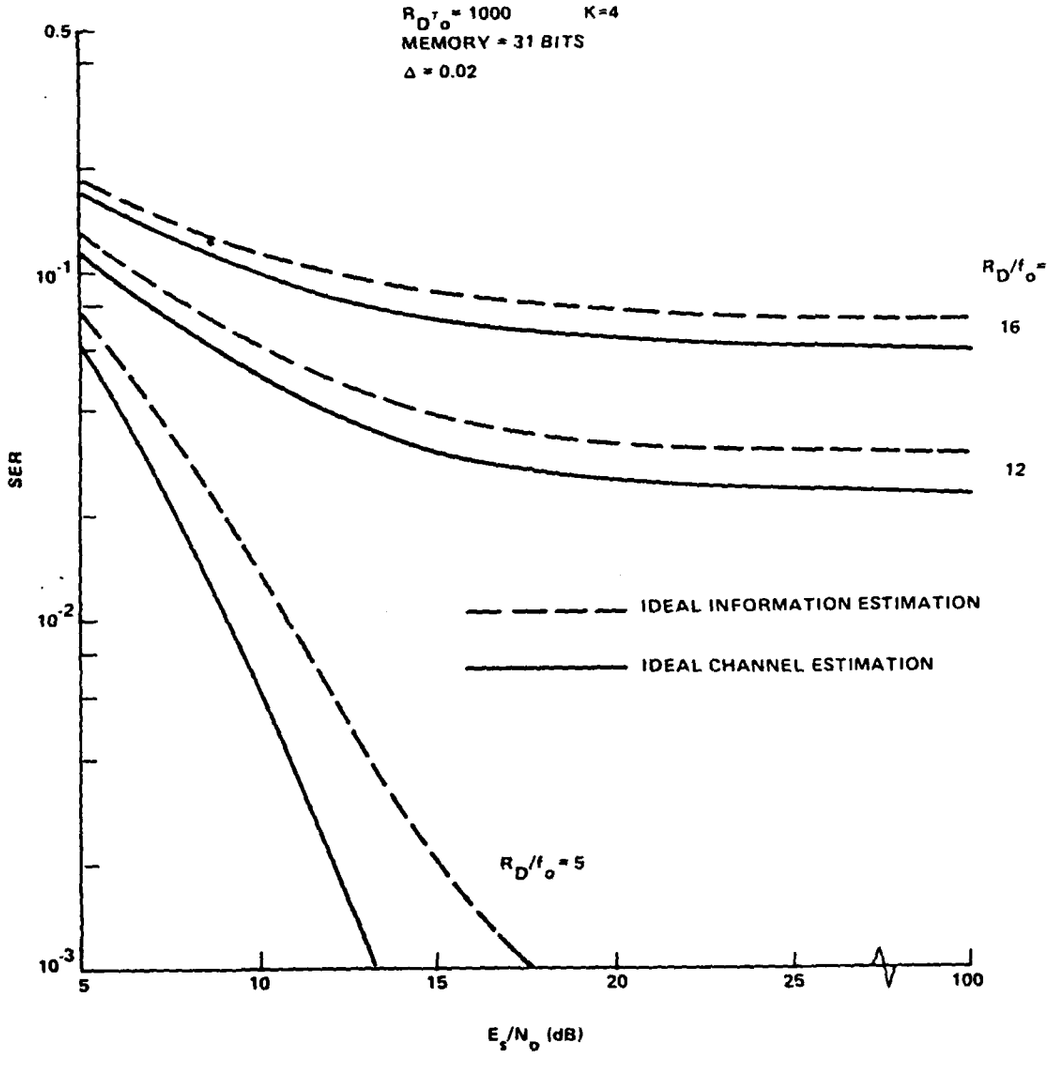

Figure 3-17 AMLSE Performance vs. E_s/N_o for K=4, Δ=0.02, and Time-Varying Channel

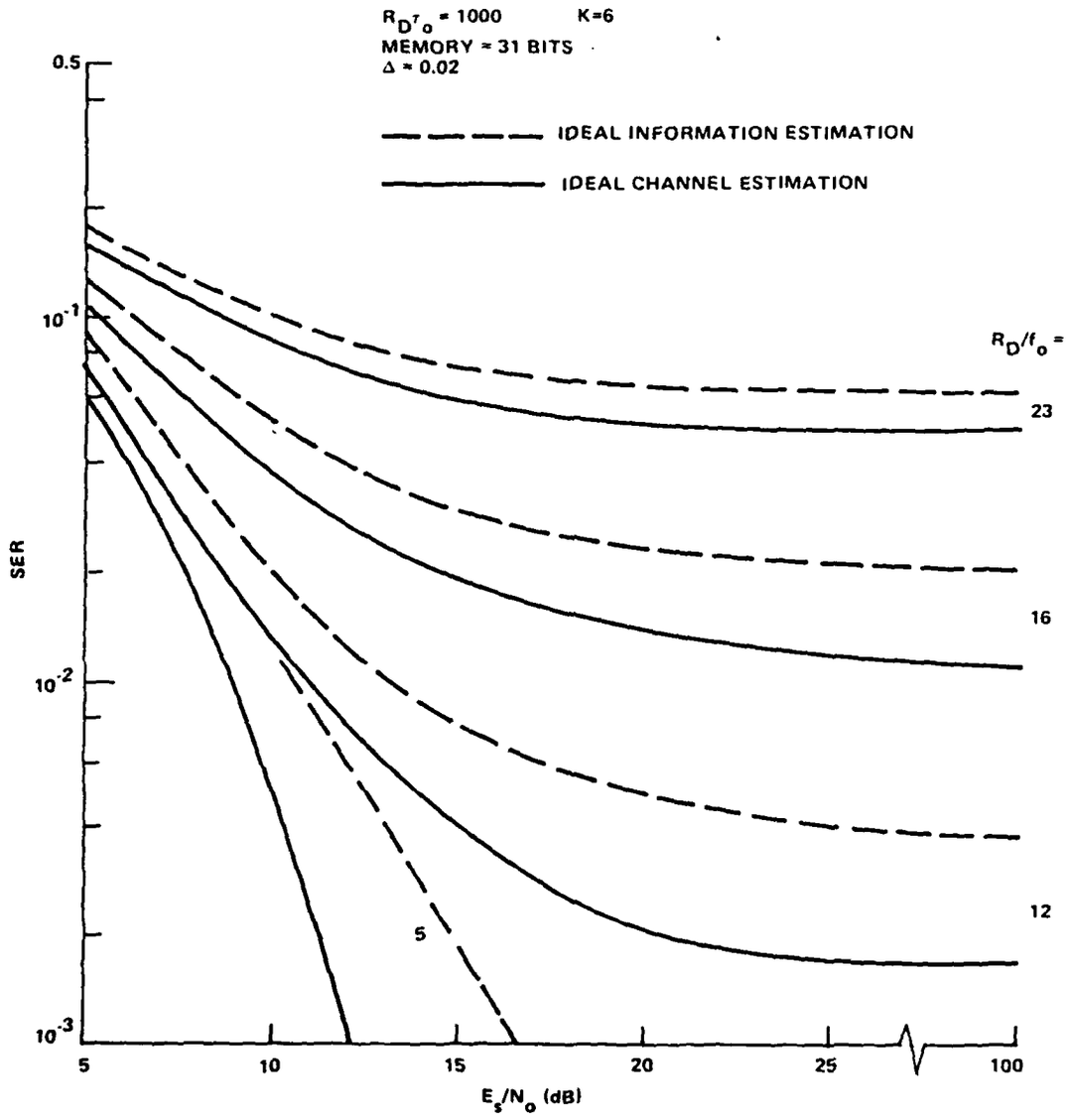

Figure 3-18 AMLSE Performance vs. E_s/N_o for K=6 Δ=0.020, and Time-Varying Channel

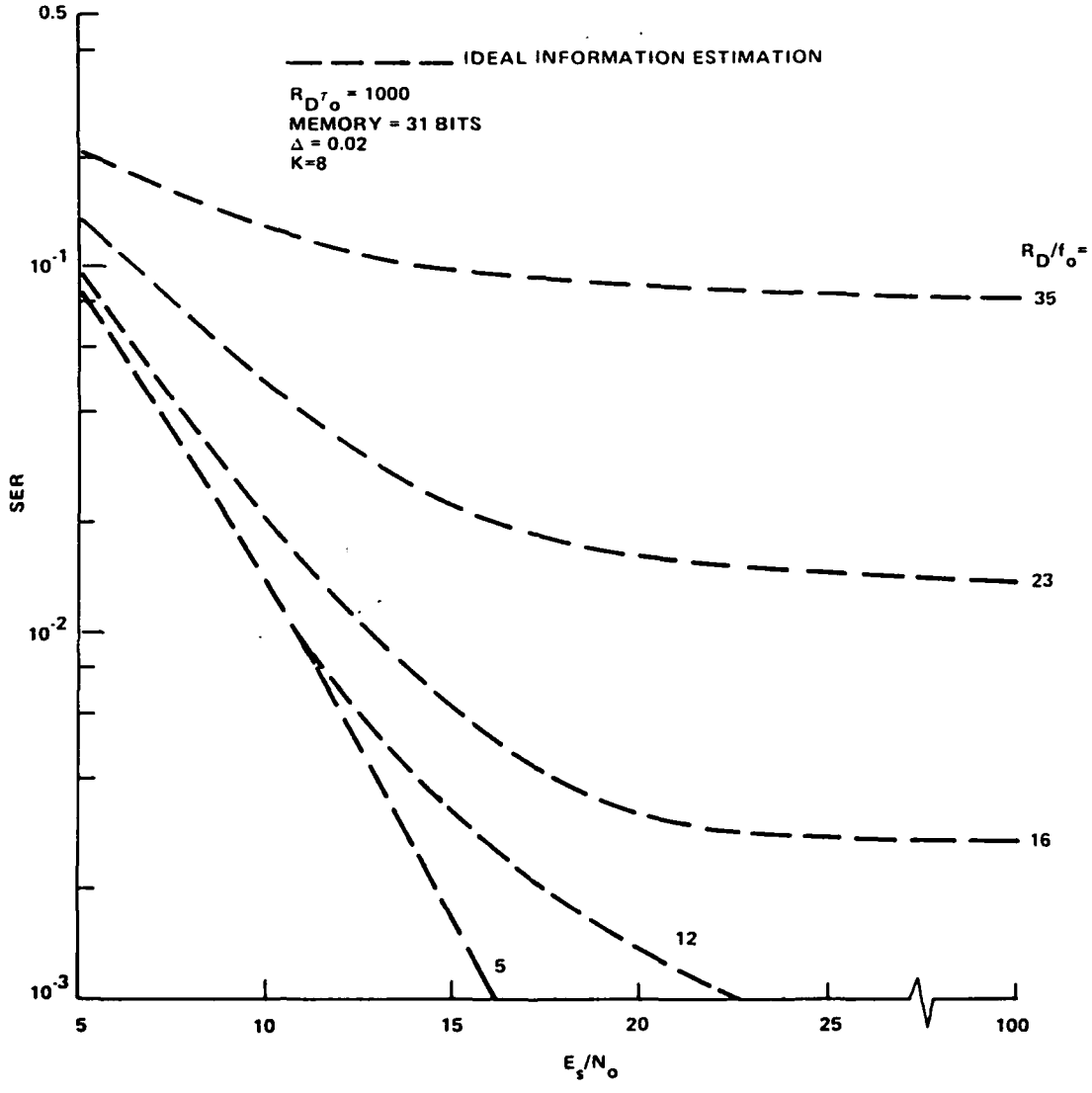

Figure 3-19 AMLSE Performance vs. E_s/N_o for K=8 Δ=0.020, and Time-Varying Channel

A block diagram showing the basic operational features of this equalization technique is shown in Figure 3-20. The basic concept employed in this channel equalizer is to truncate the longer channel impulse response being input to the shorter constraint length (K) Viterbi estimator by subtracting off the estimated impulse response beyond the K. The novel aspect of this technique is that the extended residual response is formed by the convolution of the channel estimator gain coefficients with appropriate ±1 bit sequence in the Viterbi path memory for the currently selected state rather than with a delay line symbol by symbol hard decision as is done for normal decision feedback equalization.

The incorporation of the decision feedback truncation with the AMLSE considerably improved bit demodulation performance at the higher E_s/N_o values as shown in Figure 3-21. However, at lower SNR's the AMLSE/DFE conbination actually degraded performance slightly. This effect occurs because as the SNR becomes low any channel fade will cause a longer data error burst. This in turn inputs errors into the pre-filter and results in excessive pre-filter noise into the Viterbi. The actual value of adding the DFE option to the AMLSE receiver will be determined by the SNR available and the symbol error rate (SER) operating point of the error correction coding which might be used subsequently.

Comparisons of the SER performance of the composite AMLSE/DFE equalizer and the basic DFE equalizer of various shift register lengths are shown in Figures 3-22 and 3-23. Figure 3-22 shows that a combination of an AMLSE (K=4) with a pre-filter DFE (Kest=15) equalizer should be roughly equivalent in performance to a DFE ($M_f \sim 12$, $M_b \sim 11$) equalizer for an R_D/f_o ratio of 23. Doubling the Viterbi constraint length further improves AMLSE/DFE performance by more than an order of magnitude at high SNR values as shown in Figure 3-23. Note also that the K=8 AMLSE/DFE attains markedly better performance than the DFE at higher SNR's since the AMLSE can now effectively employ its "error correction" capabilities over the channel error

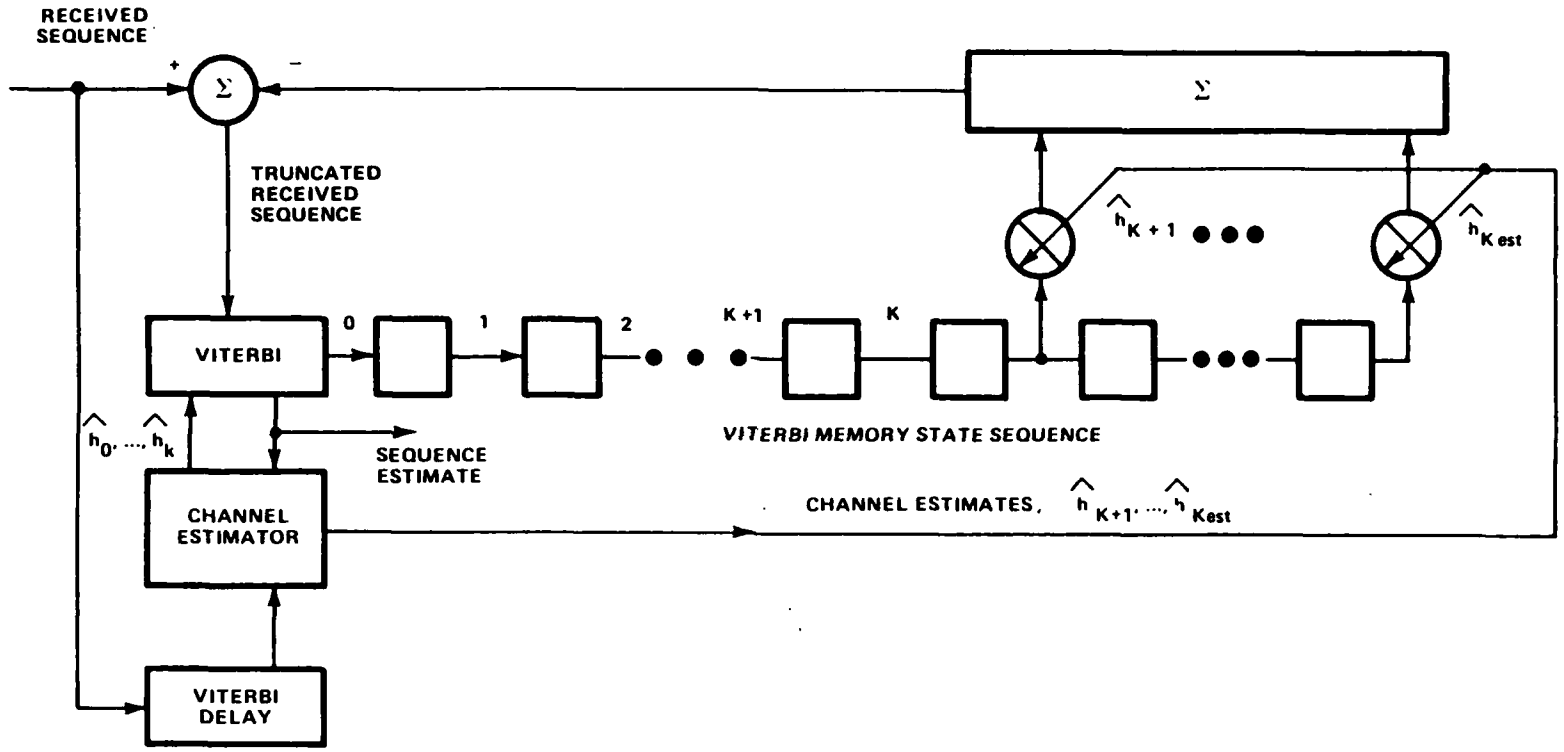

Figure 3-20 AMLSE with DFE Pre-Filter

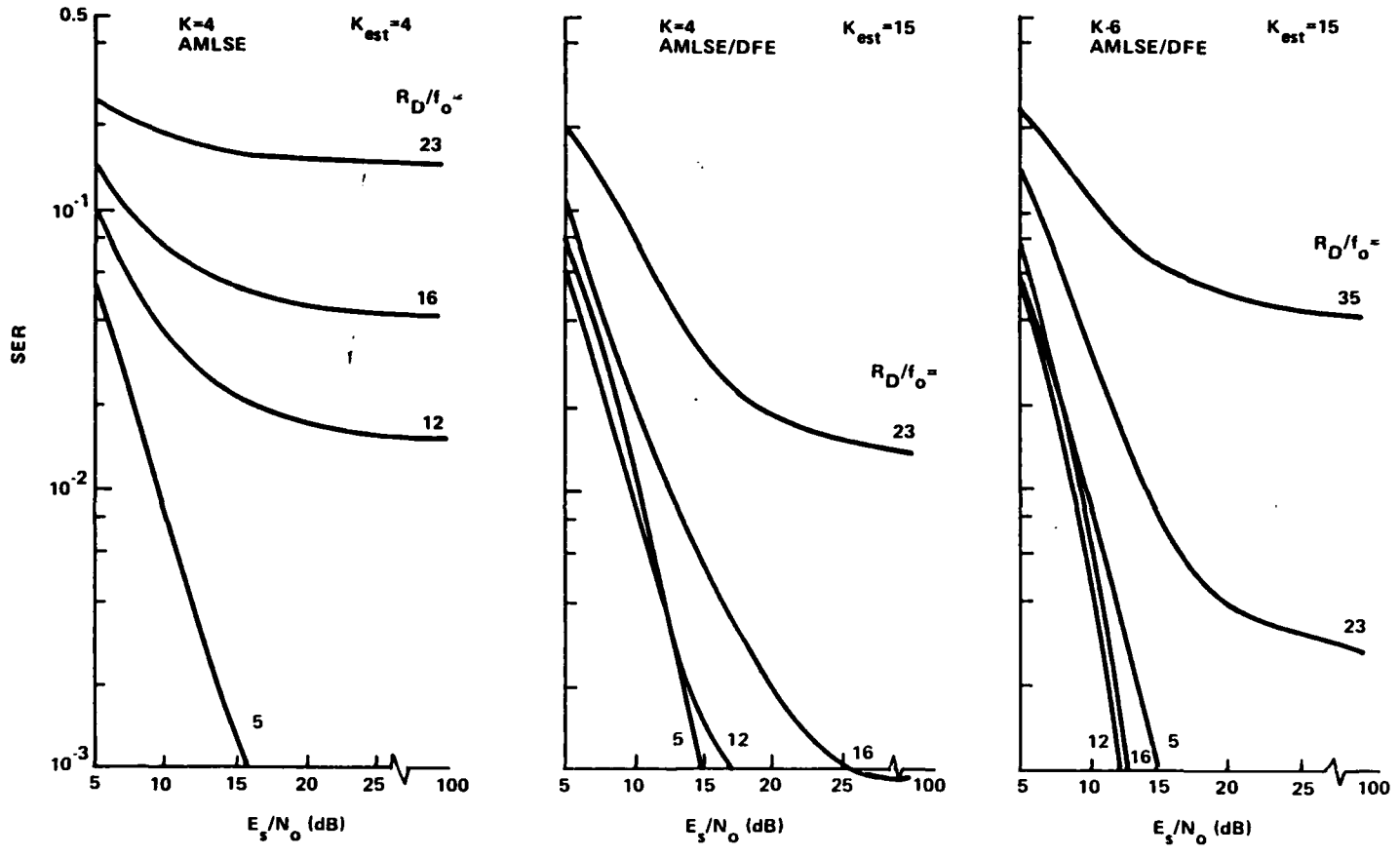

Figure 3-21 Comparison of AMLSE and AMLSE/DFE Performance for Ideal Information Aiding, $R_D\tau_o$=1000

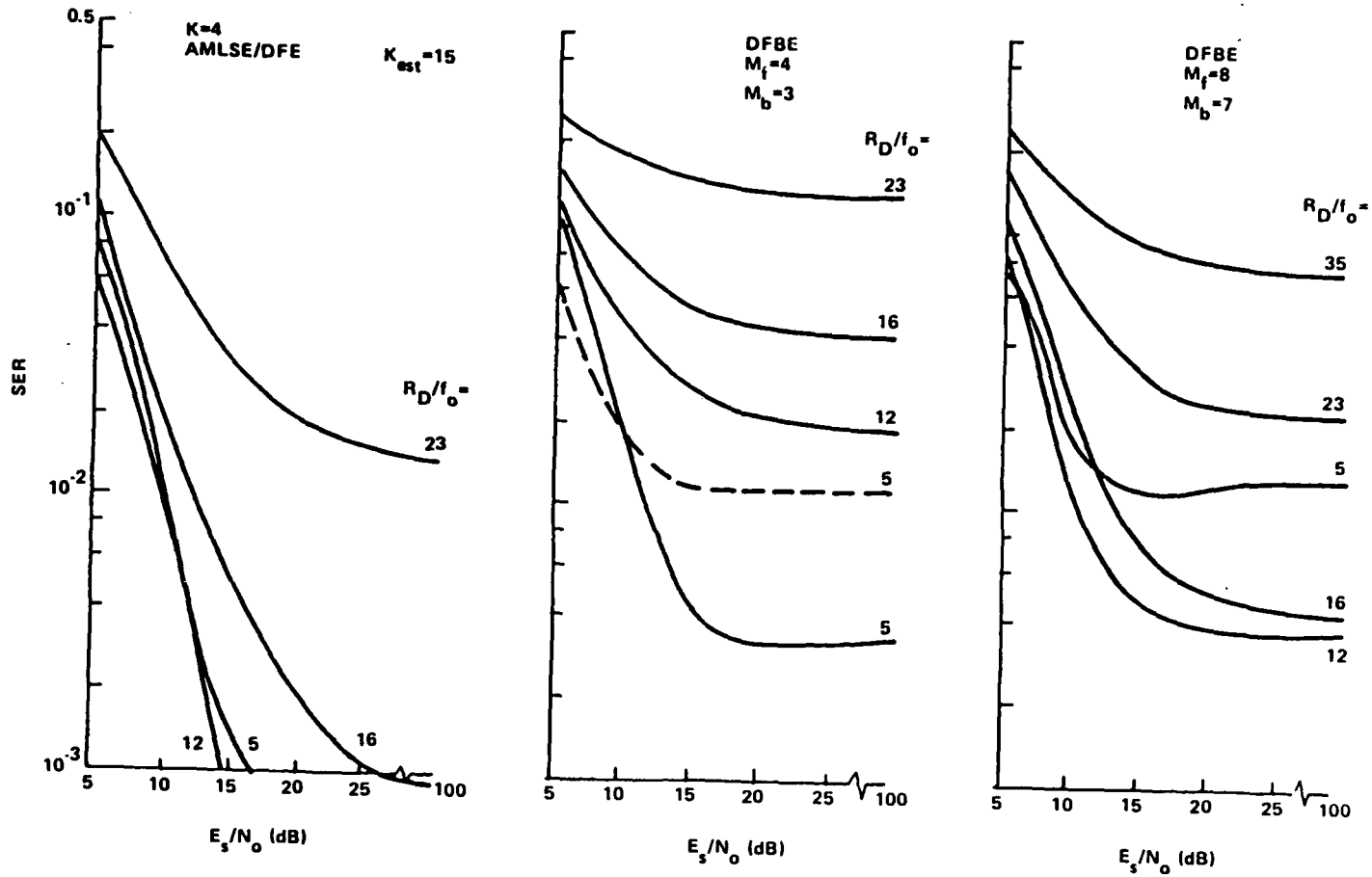

Figure 3-22 Comparison of AMLSE/DFE and DFE Performance for Ideal Information Aiding, $R_D\tau_o$=1000

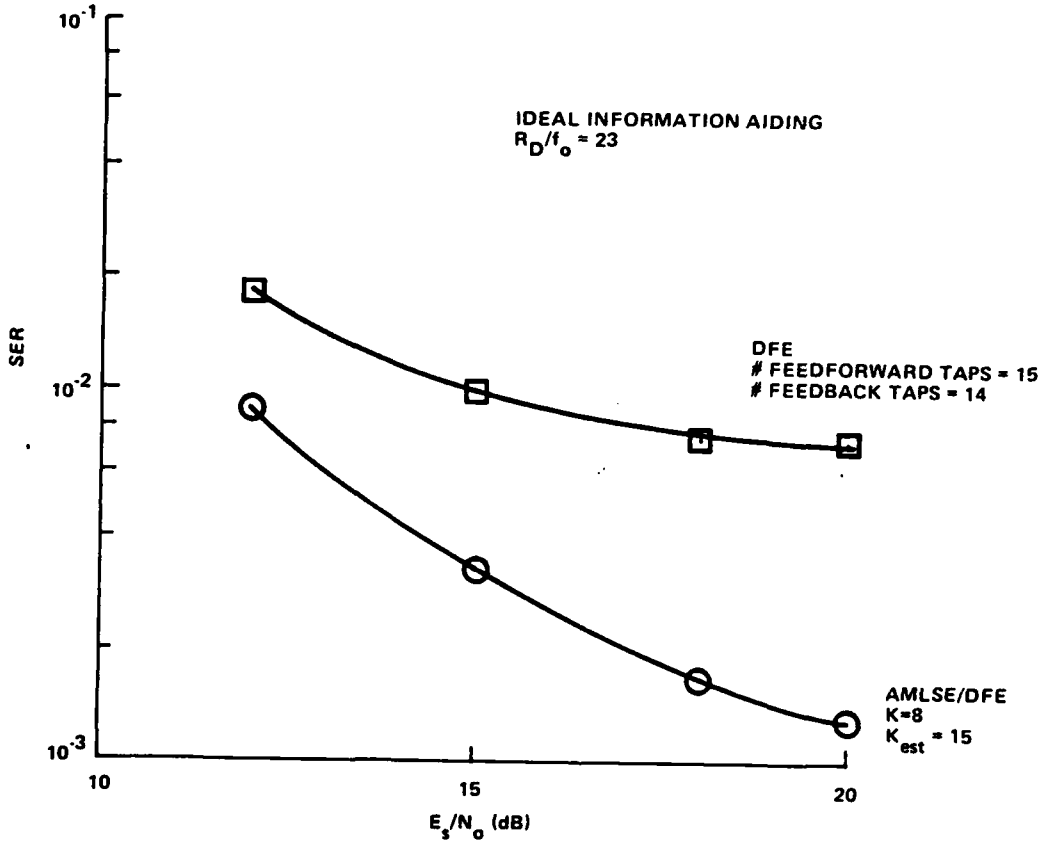

Figure 3-23 Comparison of AMLSE/DFE and DFE Performance

bursts which are shorter and fewer at higher SNR. At low SNR the channel error burst tend to overcome the AMLSE error correction capability and thus limit its performance advantage over DFE.

3.6 AMLSE/DFE PERFORMANCE WITHOUT IDEAL INFORMATION AIDING

3.6.1 Design Discussions

Up to this point, all AMLSE and Decision Feedback equalizer results presented were with ideal information aiding, i.e., perfect data was fed back to the channel estimators for the above equalizers. These idealized results allow one to obtain a lower bound on the bit error rate vs. SNR for the various equalizer configurations and also avoid a very serious problem which arose previously in the equalizer performance simulations which has to do with loss of bit synchronization.

A number of evaluations were performed to diagnose and cure the above bit slip condition so that reasonable performance can be obtained in practice without the use of unrealistically obtained ideal information aiding. These results are summarized in detail in this section. The diagnosis was based on detailed examinations of the error rates into the decision-directed channel estimator for the AMLSE, detailed evaluations of the bit error patterns, and detailed examination of the tracking behavior of the Least-Mean-Square (LMS) algorithm of the channel estimator.

In the case of the AMLSE receiver the time-varying frequency selective channel delay impulse response would fade severely at nearly all frequencies and cause a burst of errors (due to noise) in the Viterbi section of the AMLSE signal processor. This error burst would subsequently enter the decision-directed channel estimator and catastrophically degrade the impulse response estimation performance. As the channel began to recover from the fade the channel estimator (already out of lock) would start to wander in an

attempt to reacquire the impulse response and could cause a bit slip one or two bits away from the original position. Since the bit slip process occurs completely transparently with respect to the bit synchronization (it occurs after the conventional bit sync) the receiver bit synchronizer would not be expected to "track" this phenomenon. However, methods to "feedback" the bit energy delay information back to the bit sync would be of interest in further studies.

The channel estimator performance is adversely affected by the burst errors from the Viterbi decoder, and thus it was decided that an increase in the decoder "Constraint Length" was necessary. Previously, the constraint length (K) was kept low for the range of frequency decorrelation times or channel impulse dispersion lengths due to a desire to maintain AMLSE complexity and processing times on the order of the Decision Feedback Equalizer to permit a fair comparison. A data rate to frequency coherence (R_D/f_o) ratio of 16 was chosen as producing a sufficiently severe channel dispersion and a rapid decorrelation time data rate product ($R_D\tau_o$=1000) was chosen to stress the LMS convergence and acquisition capabilities of the channel estimator.

Real estimated (non-ideal) information aided simulations performed with K=4 (with R_D/f_o=16) exhibited frequent bit slip phenomena and the error rates could not be decreased to less than 10 to 20 percent or so even for large SNR values. These relatively high error rates were the result of the bit errors that occurred (after a bit slip) due to the non-allignment of the frames of data. No assumption of frame sync bits was made, though, the existence of these bits would re-sync the system and limit errors those frames where the slip actually occurred. No significant improvement occurred until the K value was increased to 7 and 8 at which point the bit slip phenomena became somewhat rare and mostly occurred for very low error rates or very severe fade samples. These results indicated that the constraint length had to be at least roughly the length of the channel impulse to effect satisfactory demodulation of the data to eliminate the long error bursts that could significantly degrade the channel estimator "lock" performance.

Another important performance aspect of a practical AMLSE configuration is its "robustness", i.e., its behavior for not only severe frequency selective fading (R_D/f_o=16 using a K=8 AMLSE configuration), but also for flat fading with R_D/f_o of much less than one. Using a K=8 AMLSE configuration, the flat fading caused frequent bit slips. Further investigation in decreasing the K to 1 resulted in elimination of the bit slips under flat fading conditions. Unfortunately it is very difficult to change the Viterbi decoder in response to changing channel dispersion lengths, however, interesting method of overcoming difficulty was subsequently derived. One can change the K value adaptively by simply controlling the channel estimator impulse input to the Viterbi decoder. Thus, the channel estimator essentially "configures" the Viterbi decoder reference response (and effective constraint length) as a function of the time-varying channel. Furthermore, one can estimate the channel impulse response length by thresholding the estimator tap values and thereby set the Viterbi decoder K to the desired value. Thus, a Viterbi decoder could be built with a capacity to handle large ranges in the channel dispersion, say from flat to highly selective, and the channel estimator would normally adaptively tailor the impulse response length to be sent to the Viterbi decoder (it would operate with the largest number of channel spread taps expected).

In addition to the "channel matching" condition required of the Viterbi constraint length or K value, it was found that the performance of the channel estimator circuit was also crucial in the optimization of the AMLSE receiver for the environments of interest. As an example, suppose that the length of the channel impulse response obtained by the channel estimator (Kest) was 6 taps longer than the K value of the decoder (Kest = K+6). The AMLSE receiver was designed to pass the first K impulse response taps to the Viterbi and subtract the response of the 6 "extra taps" from the signal into the Viterbi. This process was intended to eliminate the extra intersymbol interference (from the 6 taps) that was unmodelled in the Viterbi decoder algorithm (i.e., the K limitation). This receiver configuration is shown

in Figure 3-24. Note that the 6 tap "pre-filter" is essentially a portion of a decision feedback equalizer, however the decisions are tentatively made from the Viterbi decoder. Simulations have shown that the AMLSE/DFE equalizer enhances performance significantly at high SNR where the performance is limited by the residual or unmodelled channel impulse caused intersymbol interference.

One potential problem with the AMLSE/DFE is that due to the time-varying nature of the channel there are instances in which the channel fades away at all its "taps", thus the AMLSE/DFE decoder and the intersymbol interference "removal" would in fact be merely a noise addition process which would in turn degrade the Viterbi decoding process. A burst error output would be a highly likely result which would be feedback to the channel estimator and catastrophic error propagation conditions might arise. The existence of high SNR conditions, as mentioned earlier, can alleviate this problem since at higher SNR the fades must be deeper to cause a similar effect and deeper fades occur less often which results in better overall decoding performance. Finally, simulation results have verified that in many cases when the DFE pre-filter is utilized prior to the Viterbi decoder the occurence of bit slips due to decoder error bursts is more likely.

3.6.2 Simulation Results

Before simulation symbol error rate performation predictions are presented, it should be noted that the channel phenomenon whereby all delay taps fade simultaneously to yield a low total delay integrated power is relatively rare, however its probability of occurence effectively controls the overall performance of the receiver. This happens due to the sophisticated near-optimum decoding of the intersymbol interference by the AMLSE which results in nearly error-free performance other than for the "rare" concurrent channel tap fades. Even the running of approximately 100 to 200 time decorrelations of the fading channel is not sufficient to generate a statistical confidence level that allows the accurate measure of the long term average "true" error rate. The bit error

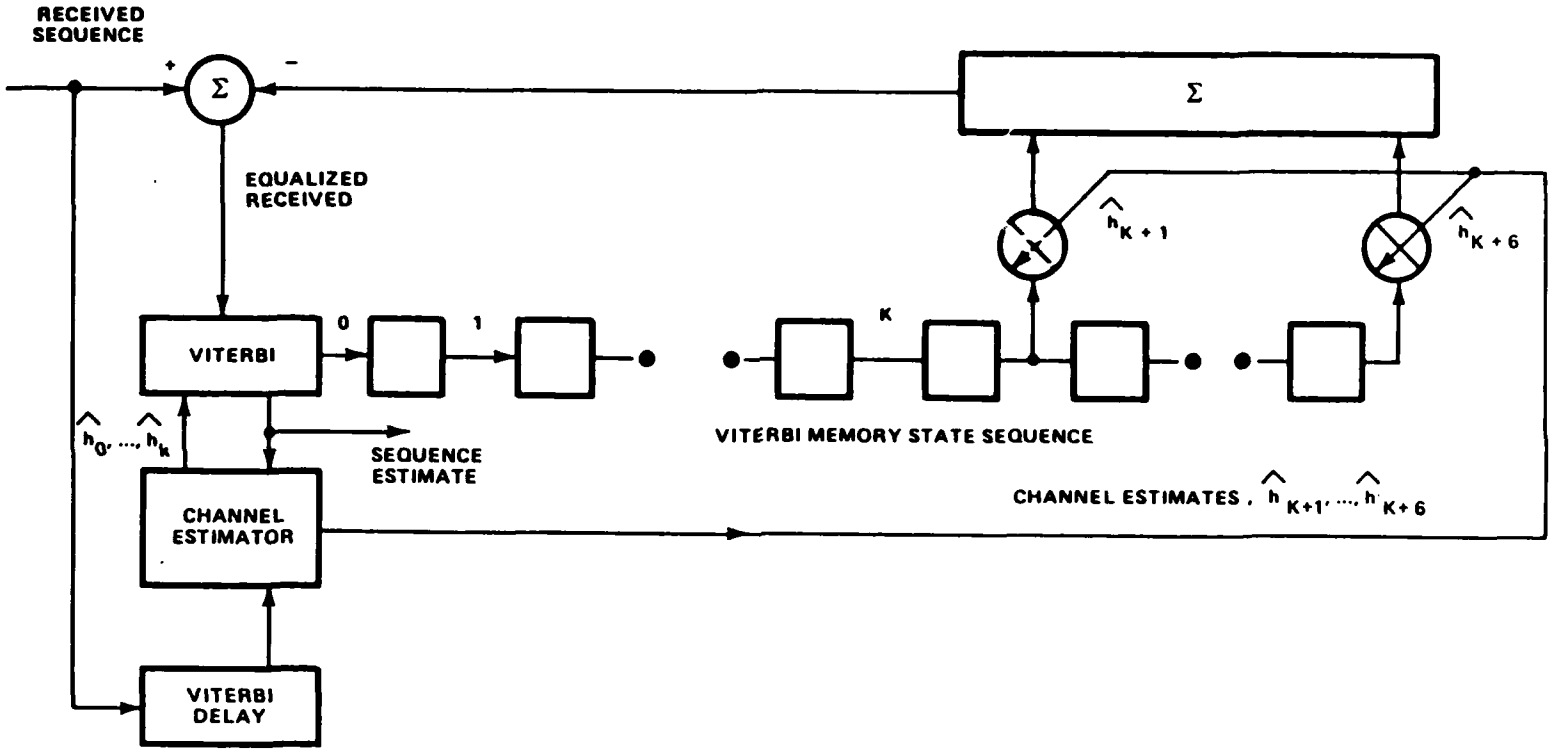

Figure 3-24 AMLSE Intersymbol Decoder Configuration

rate has been seen to vary over as much as two orders of magnitude (for a fixed SNR) depending on the particular "hundred decorrelation time" records that are run to generate accurate estimates of long term average bit error rates. Thus, the simulation results presented also have the ideal information bounds accompanying them so that the performance relative to the lower bound for the particular channel record is presented. Thus, the "closeness" of the bit error rate performance to the lower bound is of interest rather than absolute error rate.

Figure 3-25 shows simulation results for an unaided K=8 AMLSE/DFE receiver with Kest=15 for two different fading records with an R_D/f_o of 16. Note that the unaided results vary from 1 to 7 dB worse than the ideal information aided lower bound for the same configuration, nevertheless, the results are far superior to receivers that cause bit slips for which the error rates are typically 10 to 20 percent independent of SNR. Also shown for comparison is the performance for flat fading (R_D/f_o=1) for a K=1 AMLSE without DFE pre-filtering. This result suggests that the selective fading used in concert with the AMLSE processing provides some diversity gain over the flat fading result.

The performance of the best unaided Decision Feedback Equalizer (DFE) obtained thus far is also shown for comparison. The receiver configuration investigated consisted of from 7 to 15 feedforward taps and 7 to 15 feedback taps (all configurations within the above range yielded comparable performance for R_D/f_o=16) and was additionally aided by the presence of a periodic retraining sequence of known symbols which occurred 10 percent of the time and lasted for 64 symbols per occurrence. Note that unlike the DFE the AMLSE did not require any training sequence to attain its clearly superior performance.

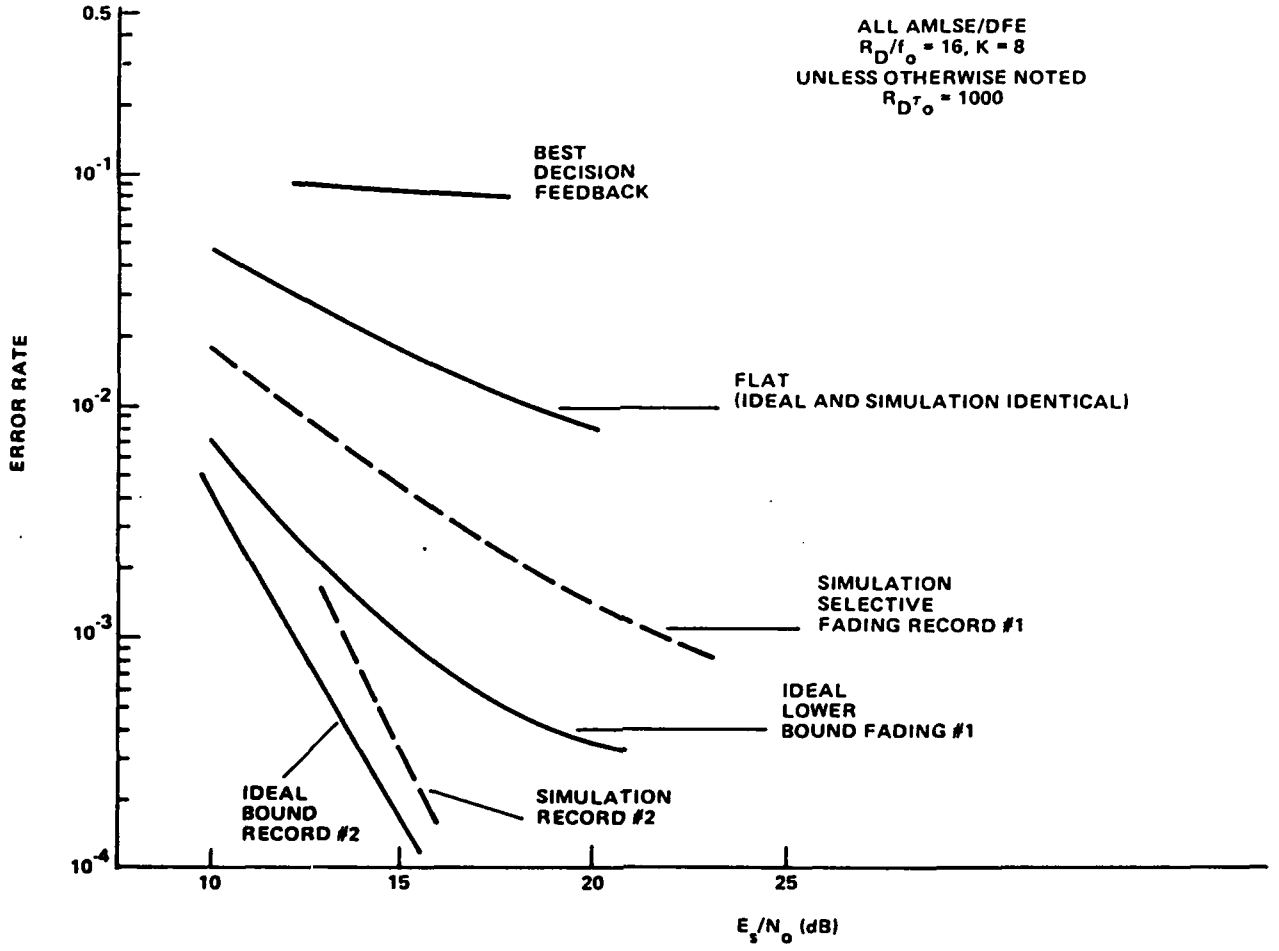

Figure 3-25 Simulation Performance of AMLSE/DFE (unaided) vs. Decision Feedback Equalization (aided with training sequences)

REFERENCES

[1] L. Wittwer, A Trans-ionospheric Signal Specification for Satellite C^3 Applications, DNA 5662D, 31 December 1980.

[2] R. W. Lucky, "Automatic Equalization for Digital Communication", Bell System Technical Journal (BSTJ)

[3] E. Satorius and J. Pack, "Application of Least-Squares Lattice Algorithms to Adaptive Equalization", IEEE Trans Commun., Vol. COM-29, February 1981, PP. 136-142.

[4] C. A. Belfiore and J. Park, "Decision Feedback Equalization", Proc. IEEE, August 1979, pp. 1143-1156.

[5] D. Falconer and F. Magee, "Adaptive Channel Memory Truncation for Maximum-Likelihood Sequence Estimation", BSTJ, Vol. 52, No. 9, November 1973, pp. 1541-1562.

[6] S. Qureshi and E. Newhall, "An Adaptive Receiver for Data Transmission Over Time-Dispersive Channels", IEEE Trans. on Info. Theory, Vol. IT-19, No. 4, July 1973, pp. 448-457.

[7] J. Proakis, "Advances in Equalization for Intersymbol Interference", Advances in Communication Systems, Vol. 4, Academic Press 1975.

[8] F. R. Magee and J. G. Proakis, "Adaptive Maximum-Likelihood Sequence Estimation for Digital Signaling in the Presence of Intersymbol Interference", IEEE Trans. on Info. Theory, Vol. IT-19, January 1973, pp. 120-124.

[9] G. D. Forney, Jr., "Maximum-Likelihood Sequence Estimation of Digital Sequences in the Presence of Intersymbol Interference", IEEE Trans. on Info. Theory, Vol. IT-18, May 1972, pp. 363-378.

[10] W. Lee and F. Hill, "A Maximum-Likelihood Sequence Estimation with Decision-Feedback Equalization", IEEE Trans. on Commun., Vol. COM-25, No. 9, September 1977, pp. 971-979.

[11] R. Bogusch et al., "Scintillation Effects and Feedback Equalization in Satellite Links", Proc. IEEE, Vol. 71, No. 6, June 1983.

[12] S. Crozier, er al., "An Adaptive Maximum Likelihood Sequence for Wideband HF Communications", MILCOM '82, Vol. 2, pp. 29.3-1.

GLOSSARY

AGC	Automatic Gain Control
AMLSE	Adaptive Maximum Likelihood Sequence Estimation
AWGN	Additive, White, Gaussian Noise
BPSK	Binary Phase-Shift-Keying
CIRF	Channel Impulse Response Function
CPSK	Coherent Phase-Shift Keying
DD	Differential Decode
DE	Differential Encode
DECPSK	Differentially Encoded Coherent Phase-Shift-Keying
DFE	Decision Feedback Equalizer
f_o	a measure of channel selective bandwidth in Hertz used as input to CIRF code equal to $1/(2\pi\sigma_\tau)$, where σ_τ = rms channel time delay spread
FSF	Frequency-Selective Fading
ICE	Ideal Channel Estimation
IIE	Ideal Information Estimation
I,Q	In-Phase, Quadrature
ISI	Intersymbol interference
K	Constraint length of Viterbi decoder
LMS	Least Mean Square
LO	Local Oscillator
M_B	Number of feedback taps of Decision Feedback Equalizer
M_F	Number of feedforward taps of Decision Feedback Equalizer
PLL	Phase-locked loop
PN	Pseudo-random noise
R_D	data rate
$R_D\tau_o$	data rate-decorrelation time product
τ_o	e^{-1} decorrelation time of the fading temporal covariance function in seconds
SER	Symbol Error Rate
TDL	tapped delay line
Δ	convergence constant or coefficient of Adaptive Channel Estimator

DISTRIBUTION LIST

DEPARTMENT OF DEFENSE

Command & Control Tech Ctr
ATTN: C-650, G. Jones
ATTN: C-650
ATTN: C-312, R. Mason
3 cy ATTN: C-650, W. Heidig

Defense Communications Agency
ATTN: Code 205
ATTN: Code 230
ATTN: J300 for Yen-Sun Fu

Defense Communications Engrg Ctr
ATTN: Code R123
ATTN: Code R410, N. Jones
ATTN: Code R410

Defense Nuclear Agency
ATTN: NATD
ATTN: RAEE
ATTN: STNA
ATTN: NAFD
3 cy ATTN: RAAE
4 cy ATTN: TITL

Defense Tech Info Ctr
12 cy ATTN: DD

WWMCCS System Engrg Org
ATTN: J. Hoff

DEPARTMENT OF THE ARMY

BMD Advanced Tech Ctr
ATTN: ATC-R, W. Dickinson
ATTN: ATC-R, D. Russ
ATTN: ATC-T, M. Capps
ATTN: ATC-O, W. Davies

BMD Systems Command
ATTN: BMDSC-HLE, R. Webb
2 cy ATTN: BMDSC-HW

US Army Communications Command
ATTN: CC-OPS-WR, H. Wilson
ATTN: CC-OPS-W

US Army Satellite Comm Agency
ATTN: Doc Con

US Army Nuc & Chem Agency
ATTN: Library

DEPARTMENT OF THE NAVY

Naval Electronic Systems Cmd
ATTN: PME 117-211, B. Kruger
ATTN: PME 106-4, S. Kearney
ATTN: PME 106, F. Diederich
ATTN: PME 117-2013, G. Burnhart
ATTN: PME 117-20
ATTN: Code 3101, T. Hughes
ATTN: Code 501A

Naval Space Surveillance System
ATTN: J. Burton

DEPARTMENT OF THE NAVY (Continued)

Naval Ocean Sys Ctr
ATTN: Code 5322, M. Paulson
ATTN: Code 532
ATTN: Code 5323, J. Ferguson

Naval Rsch Lab
ATTN: Code 4780, S. Ossakow
ATTN: Code 4108, E. Szuszewicz
ATTN: Code 4720, J. Davis
ATTN: Code 6700
ATTN: Code 7950, J. Goodman
ATTN: Code 4780,
ATTN: Code 7500, B. Wald
ATTN: Code 4187
ATTN: Code 4700

Naval Surface Weapons Ctr
ATTN: Code F31

Naval Telecomm Cmd
ATTN: Code 341

Office of Naval Rsch
ATTN: Code 414, G. Joiner
ATTN: Code 412, W. Condell

Strat Sys Project Ofc
ATTN: NSP-2722
ATTN: NSP-2141
ATTN: NSP-43

DEPARTMENT OF THE AIR FORCE

Air Force Geophysics Lab
ATTN: LYD, K. Champion
ATTN: OPR-1
ATTN: R. Babcock
ATTN: CA, A. Stair
ATTN: OPR, H. Gardiner
ATTN: PHY, J. Buchau
ATTN: R. O'Neil

Air Force Tech Applications Ctr
ATTN: TN

Air Force Weapons Lab
ATTN: SUL
ATTN: NTN

Air Force Wright Aeronautical Lab, AAAD
ATTN: W. Hunt
ATTN: A. Johnson

Air University Library
ATTN: AUL-LSE

Assistant Chief of Staff
Studies & Analysis
ATTN: AF/SASC, C. Rightmeyer

Foreign Tech Div
ATTN: TQTD, B. Ballard
ATTN: NIIS Library

DEPARTMENT OF THE AIR FORCE (Continued)

Electronic Systems Div
ATTN: ESD/SCTE, J. Clark

Rome Air Dev Ctr
ATTN: OCS, V. Coyne
ATTN: OCSA, R. Schneible
ATTN: TSLD

Rome Air Dev Ctr
ATTN: EEPS, P. Kossey
ATTN: EEP, J. Rasmussen

Space Command
ATTN: DC, T. Long

Strat Air Cmd
ATTN: ADWA
ATTN: XPQ
ATTN: XPFC
ATTN: DCX
ATTN: DCZ
ATTN: NRI/STINFO Library
ATTN: XPFS

OTHER GOVERNMENT AGENCIES

Central Intelligence Agency
ATTN: OSWR/NED
ATTN: OSWR/SSD for K. Feuerpfetl

National Bureau of Standards
ATTN: Sec Ofc for R. Moore

National Oceanic & Atmospheric Admin
ATTN: R. Grubb

Institute for Telecomm Sciences
ATTN: W. Utlaut
ATTN: A. Jean
ATTN: L. Berry

DEPARTMENT OF ENERGY CONTRACTORS

Sandia National Labs
ATTN: Tech Lib 3141
ATTN: Org 1250, W. Brown
ATTN: Org 4231, T. Wright
ATTN: D. Thornbrough
ATTN: Space Project Div
ATTN: D. Dahlgren

DEPARTMENT OF DEFENSE CONTRACTORS

Aerospace Corp
ATTN: D. Olsen
ATTN: I. Garfunkel
ATTN: J. Ailey
ATTN: J. Kluck
ATTN: D. Whelan
ATTN: R. Slaughter
ATTN: J. Straus
ATTN: K. Cho
ATTN: V. Josephson
ATTN: T. Salmi

Analytical Systems Engrg Corp
ATTN: Radio Sciences

DEPARTMENT OF DEFENSE CONTRACTORS (Continued)

Analytical Systems Engrg Corp
ATTN: Security

BDM Corp
ATTN: T. Neighbors
ATTN: L. Jacobs

Berkeley Rsch Associates, Inc
ATTN: J. Workman
ATTN: C. Prettie
ATTN: S. Brecht

Charles Stark Draper Lab, Inc
ATTN: D. Cox
ATTN: A. Tetewski
ATTN: J. Gilmore

ESL, Inc
2 cy ATTN: R. Ibaraki
2 cy ATTN: E. Tsui
2 cy ATTN: J. Hawker

GTE Communications Products Corp
ATTN: I. Kohlberg
ATTN: J. Concordia

Harris Corp
ATTN: E. Knick

Institute for Defense Analyses
ATTN: H. Gates
ATTN: J. Aein
ATTN: E. Bauer
ATTN: H. Wolfhard

International Tel & Telegraph Corp
ATTN: Tech Library

Kaman Tempo
ATTN: DASIAC
ATTN: B. Gambill
ATTN: W. Schuleter
ATTN: W. McNamara

Kaman Tempo
ATTN: DASIAC

M/A Com Linkabit Inc
ATTN: H. Van Trees
ATTN: I. Jacobs
ATTN: A. Viterbi

Magnavox Govt & Indus Elec Co
ATTN: G. White

Mission Rsch Corp
ATTN: R. Bogusch
ATTN: F. Fajen
ATTN: S. Gutsche
ATTN: R. Hendrick
ATTN: Tech Library
ATTN: F. Guigliano
ATTN: G. McCartor
ATTN: R. Bigoni
ATTN: R. Dana
ATTN: R. Kilb
ATTN: D. Knepp
4 cy ATTN: C. Lauer

DEPARTMENT OF DEFENSE CONTRACTORS (Continued)

Pacific-Sierra Rsch Corp
ATTN: H. Brode, Chairman SAGE

Physical Rsch Inc
ATTN: R. Deliberis
ATTN: T. Stephens
ATTN: J. Devore

R&D Associates
ATTN: W. Wright
ATTN: R. Turco
ATTN: G. Stcyr
ATTN: W. Karzas
ATTN: M. Gantsweg
ATTN: F. Gilmore
ATTN: C. Griefinger
ATTN: H. Ory
ATTN: P. Haas

R&D Associates
ATTN: B. Yoon

Physical Dynamics, Inc
ATTN: E. Fremouw
ATTN: J. Secan

DEPARTMENT OF DEFENSE CONTRACTORS (Continued)

SRI International
ATTN: A. Burns
ATTN: G. Price
ATTN: R. Tsunoda
ATTN: J. Vickrey
ATTN: V. Gonzales
ATTN: J. Petrickes
ATTN: M. Baron
ATTN: R. Livingston
ATTN: D. Neilson
ATTN: D. McDaniels
ATTN: W. Chestnut
ATTN: G. Smith
ATTN: W. Jaye
ATTN: R. Leadabrand
ATTN: C. Rino

Rand Corp
ATTN: E. Bedrozian
ATTN: P. Davis
ATTN: C. Crain

GTE Communications Products Corp
ATTN: R. Steinhoff

fade the channel estimator (already out of lock) would start to wander in an